UNIVERSITÀ DEGLI STUDI DI PALERMO

Dottorato di Ricerca in Biomedicina e Neuroscienze

Dipartimento di Biomedicina, Neuroscienze e Diagnostica avanzata

SSD BIO/16

Impact of cigarette smoke on inflammasome-dependent responses in human lung fibroblasts

IL CANDIDATO

Agnese La Mensa

Matricola 0724493

IL COORDINATORE

Prof. Fabio Bucchieri

IL TUTOR

Prof. Fabio Bucchieri

IL CO-TUTOR

Dr. Chiara Cipollina

CICLO XXXVI

ANNO CONSEGUIMENTO 2022-2023

Table of Contents

Introduction

1. Cigarette smoke and chronic obstructive pulmonary disease (COPD)

Chronic Obstructive Pulmonary Disease (COPD) is a common and persistent airway disease associated with limitation in airflow. According to the Global Burden of Disease Study 2019, the global prevalence of COPD was estimated to be 10.3% in 2019, accounting for 391.9 million cases among people aged 30-79 years. In 2015, COPD was responsible for 3.2 million deaths worldwide, making it the third leading cause of death, especially in low- and middle-income countries[1–4]. COPD is caused by prolonged exposure to harmful particles or gases, with cigarette smoke (CS) being the most common cause worldwide. This is a complex disease associated with abnormalities of the airway and/ or alveoli [5].

This burden is predicted to grow due mainly to increased global exposure to tobacco, aging populations, poor awareness, and inadequate access to diagnosis. COPD exacerbations are a major event in the natural history of the disease associated with worsening of symptoms often resulting in hospitalization and poor prognosis[6]. COPD is characterized by chronic lung inflammation that culminates in progressive and irreversible airflow obstruction.

Although cigarette smoke is considered the principal predisposing risk factor for the development of COPD, not all smokers develop this disease, indicating that other environmental factors and genetic susceptibility could contribute to the development of this disease [7].

The relationship between COPD and smoking is well-established, but its molecular underpinnings remain a subject of intense scientific scrutiny. Tobacco smoke is a complex mix of thousands of chemicals, many of which are toxic and carcinogenic[8]. When inhaled, these constituents initiate a cascade of events within the respiratory system that ultimately lead to chronic inflammation and structural damage. Exposure to cigarette smoke contributes to the pathogenesis of various disorders.

CS exposure damages the epithelial barrier and impairs its function. Lung fibroblasts are highly susceptible to oxidative stress, which can trigger their activation and differentiation into myofibroblasts, thereby contributing to tissue remodeling and fibrosis. It induces histological changes such as epithelial remodeling and sub-epithelial fibrosis of the small airways, damages proteins and organelles via oxidative stress, and causes accelerated lung aging: this may contribute to the development and/or progression of COPD [9,10] .

2. Innate immunity and inflammasomes in COPD

Innate immunity serves as the body's first line of defense against pathogens and environmental challenges. Its components, which include physical barriers like the skin, and bronchial mucosa, chemical defenses like stomach acid, and cellular elements like macrophages and neutrophils, are always at the ready to detect and neutralize potential threats[11]. Within the respiratory system, the innate immune response is particularly critical due to the constant exposure of the airways to inhaled particles, microorganisms, and pollutants. The lungs, with their vast surface area, are constantly under assault from the external environment, and thus, a robust and finely tuned innate immune response is essential for maintaining respiratory health[12].

In COPD, the intricate balance of innate immunity is disrupted, leading to chronic inflammation and tissue damage. Neutrophils, macrophages, and other immune cells are increased and display altered function in cigarette smoke-associated inflammation and COPD[13]. While their arrival is a critical defense mechanism against potential infections, the prolonged activation of these cells and defective resolution mechanisms can result in collateral damage to lung tissue. The innate immune response in COPD is marked by an overproduction of pro-inflammatory cytokines, such as tumor necrosis factor-alpha (TNF), interleukin-1β (IL-1β), interleukin-18 (IL-18) and interleukin-6 (IL-6). These molecules further fuel the inflammatory process, attracting more immune cells to the site of injury and perpetuating the vicious cycle of chronic inflammation [14]. A key facet of the innate immune response lies in the activation of pattern recognition receptors (PRRs). These receptors are specialized molecules that recognize specific molecular patterns associated with pathogens, also known as pathogen-associated molecular patterns (PAMPs). In the context of COPD, PRRs play a crucial role in detecting harmful components of cigarette smoke and initiating the immune response.

One class of PRRs, Toll-like receptors (TLRs), has received significant attention in COPD research[15]. TLRs, located on the surface of immune cells but also in structural cells such as bronchial epithelial cells and fibroblasts, recognize a range of PAMPs and trigger the release of pro-inflammatory cytokines. Cigarette smoke contains PAMP-like molecules, and the sustained activation of TLRs by these cigarette smoke constituents contributes to the persistent inflammation observed in COPD[16]. The lungs are equipped with a diverse range of cellular components that act as sentinels and defenders against harmful agents in the environment. Among these, alveolar macrophages, epithelial cells, and structural cells such as lung fibroblasts play vital roles in maintaining respiratory health. When exposed to cigarette smoke, these resident cellular components recognize the toxic agents as threats and initiate an immune response. This response triggers a cascade of events that ultimately leads to inflammation and structural remodeling of the lung tissue[17]. Cigarette smoke exposure prompts resident lung cells to release a variety of signaling molecules, including cytokines and chemokines. These molecules serve as messengers of inflammation, orchestrating the recruitment and activation of immune cells to the site of injury. Cytokines such as IL-1β and IL-18 are powerful pro-inflammatory mediators, driving the chronic inflammation observed in COPD. Chemokines, on the other hand, guide immune cells to the inflamed lung tissue, promoting a sustained immune response. Recent scientific research was aimed at understanding the contribution of the NLRP3 (NOD-, LRR- and pyrin domain-containing protein 3) inflammasome to the pathogenesis of cigarette-smoke-associated lung diseases, including COPD[18,19]. The NLRP3 inflammasome is a multiprotein complex that plays a central role in the regulation of inflammatory responses. Activation of the NLRP3 inflammasome is a multi-step process[20] requiring TLR-mediated transcriptional priming followed by a second signal leading to the formation of the active complex (Fig.1). Activation of the inflammasome typically begins with the recognition of danger signals or damage-associated molecular patterns (DAMPs). In the context of cigarette smoke exposure, these DAMPs can originate from the toxic components within cigarette smoke[21]. The activated NLRP3 inflammasome, in turn, triggers the proteolytic cleavage and activation of caspase-1. Activated caspase-1 facilitates the maturation and secretion of pro-inflammatory cytokines, specifically IL-1β and IL-18. These cytokines are potent drivers of inflammation, amplifying the immune response initiated by cigarette smoke[22]. Active caspase-1, can also cleave and activate gasdermin D (GSDMD)[2324]. GSDMD is a critical mediator in the inflammatory process, as it plays a central role in

pyroptosis, a highly inflammatory form of programmed cell death. During pyroptosis, GSDMD forms pores in the cell membrane[25]. These pores allow the release of pro-inflammatory cellular contents, including cytokines and other molecules, into the extracellular space[26]. This process amplifies the inflammatory response and may contribute to the tissue damage observed in COPD.

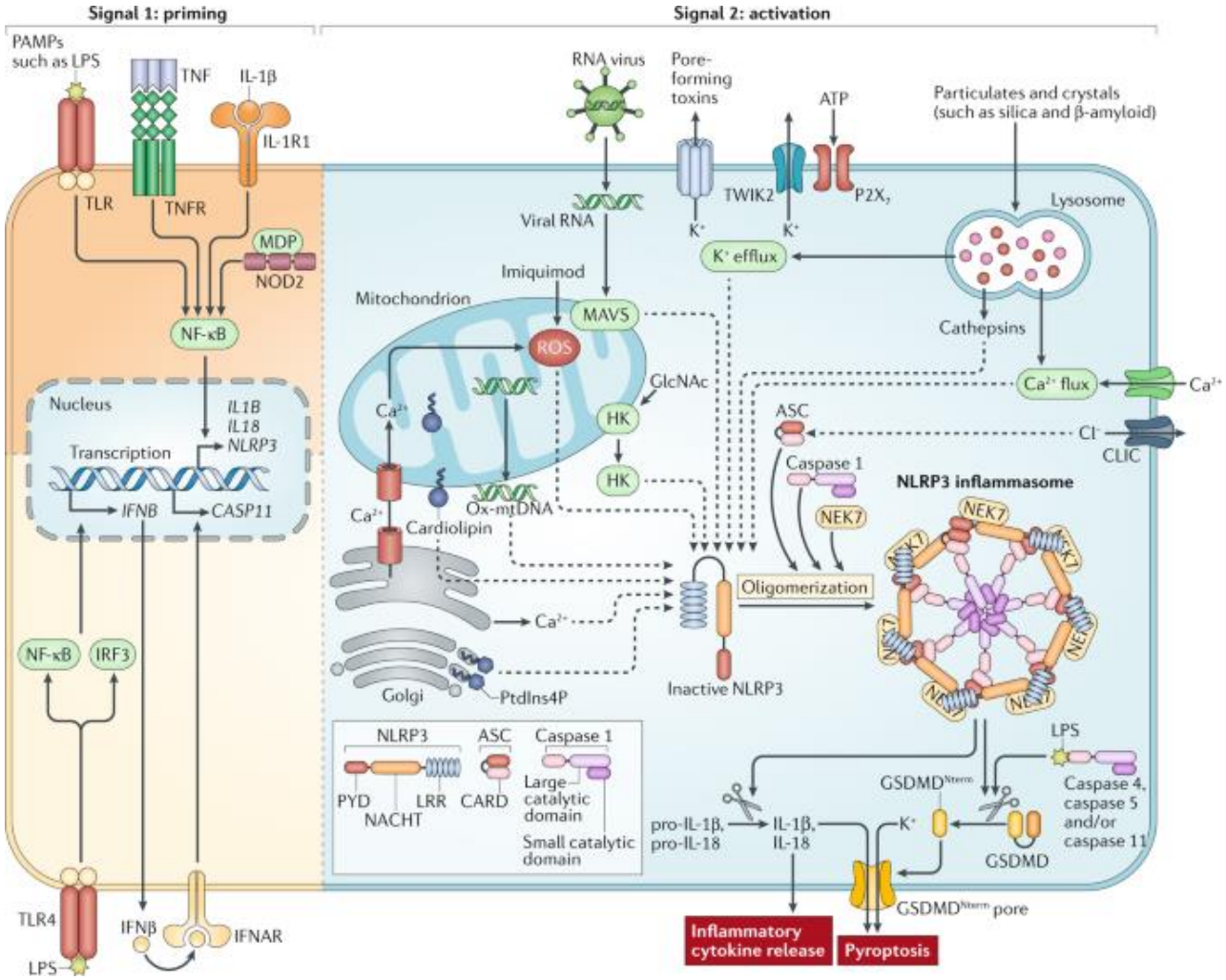

Fig. 1: NLRP3 complex and relative pathway. *The signal 1 (priming; left) is provided by the activation of cytokines or pathogen-associated molecular patterns (PAMPs), leading to the transcriptional upregulation of canonical and non-canonical NLRP3 (NOD-, LRR- and pyrin domain-containing protein 3) inflammasome components. Signal 2 (activation; right) is provided by any of numerous PAMPs or damage-associated molecular patterns (DAMPs), such as particulates, crystals and ATP, that activate multiple upstream signalling events. These include K+ efflux, Ca+ flux, lysosomal disruption, mitochondrial reactive oxygen species (mROS) production, the relocalization of cardiolipin to the outer mitochondrial membrane and the release of oxidized mitochondrial DNA (Ox-mtDNA), followed by Cl− efflux. RNA viruses activate NLRP3 through mitochondrial antiviral signalling protein (MAVS) on the mitochondrial outer membrane. Formation of the inflammasome activates caspase 1, which in turn cleaves pro-IL-1β and pro-IL-18. Gasdermin D (GSDMD) is also cleaved and inserts into the membrane, forming*

pores and inducing pyroptosis. Upon detection of cytosolic lipopolysaccharide (LPS), caspases 4, 5 and 11 are activated and cleave GSDMD, triggering pyroptosis. CARD, caspase recruitment domain; CLIC, chloride intracellular channel protein; GlcNAc, N-acetylglucosamine; GSDMDNterm, GSDMD amino-terminal cell death domain; HK, hexokinase; IFNAR, IFNα/β receptor; IL-1R1, IL-1 receptor type 1; IRF3, interferon regulatory factor 3; LRR, leucine-rich repeat; MDP, muramyl dipeptide; NEK7, NIMA-related kinase 7; NF-κB, nuclear factor-κB; P2X7, P2X purinoceptor 7; PtdIns4P, phosphatidylinositol-4-phosphate; PYD, pyrin domain; ROS, reactive oxygen species; TLR, Toll-like receptor; TNF, tumour necrosis factor; TNFR, tumour necrosis factor receptor; TWIK2, two-pore domain weak inwardly rectifying K+ channel 2.
From H.M.Blevins, 2022, Front Aging Neurosci[27].

A 2021 review article discussed the role of the NLRP3 inflammasome in the pathogenesis and treatment of COPD. The article mentioned that the systemic and local airway activity of the NLRP3 inflammasome is associated with acute exacerbation of COPD[28]. Caspase-1 is activated by the NLRP3 inflammasome and other inflammasomes in many cellular types including structural cells such as epithelial cells and fibroblasts[29]. However, the role of the NLRP3 inflammasome in cigarette smoke-related diseases is still a matter of debate and available data are limited[30–32]. Growing evidence suggests that cigarette smoke activates the NLRP3 inflammasome in the lung epithelium, with increased expression of NLRP3, pro-IL-1β and caspase-1, higher caspase-1 activity, and increased release of inflammasome-related cytokines IL-1β and IL-18[33–35]. Macrophages appear to respond differently as cigarette smoke extract exposure inhibits inflammasome activation and reduces the release of IL-1β and IL-18 [36,37]. Buscetta et al. described that in human macrophages exposed to CSE Caspase-1 is activated independently of NLRP3 via the TLR4-TRIF-caspase-8 axis [38]. Caspases are a family of cysteine proteases that are primarily known for their involvement in programmed cell death, or apoptosis. However, recent research has revealed that caspases also have non-apoptotic functions, contributing to various physiological and pathological processes and participating in inflammatory reactions [39–41]. Apoptotic and non-apoptotic caspases play crucial roles in regulating cell death and maintaining cellular homeostasis[42–44]. The non-apoptotic caspases, such as caspase-1, -4, and -5, are involved in inflammatory responses and immune regulation. Apoptotic caspases, such as caspase-3, -6, and -7, are the key executioners of apoptosis, responsible for cleaving numerous cellular substrates and ultimately dismantling the cell[45–47]. Caspase activation during apoptosis occurs through a cascade of proteolytic events, initiated by either intrinsic or extrinsic signals. Mitochondrial outer membrane permeabilization (MOMP) is a critical event in the intrinsic pathway of apoptosis, also known as the

mitochondrial apoptotic pathway. It is triggered by intracellular stresses, such as DNA damage or cellular stress, leading to the release of cytochrome c from the mitochondria and the formation of the apoptosome complex (Fig.2). MOMP is regulated by the BCL-2 family of proteins, with pro-apoptotic members, such as BAX and BAK, promoting membrane permeabilization, while anti-apoptotic members, such as BCL-2 and BCL-XL, inhibit MOMP. Once MOMP occurs, the released cytochrome c interacts with the apoptotic protease-activating factor 1 (Apaf-1) to form the apoptosome, which activates caspase-9. Caspase-9 then cleaves and activates downstream effector caspases, such as caspase-3, leading to the execution of apoptosis. In addition to caspase-9, MOMP can also lead to the activation of caspase-3 through a caspase-9-independent mechanism, involving the release of other mitochondrial factors, such as second mitochondria-derived activator of caspases (SMAC) and cytochrome c, which can promote caspase activation. Therefore, MOMP is a critical event in the intrinsic pathway of apoptosis, leading to the activation of caspases and the execution of programmed cell death [48–53]. The extrinsic pathway or death receptor pathway, on the other hand, is initiated by the engagement of death ligands, such as Fas ligand (FasL) and tumor necrosis factor alpha (TNF), and by their binding to their respective death receptors, including Fas and TNF receptor 1 (TNFR1). This binding leads to the formation of a death-inducing signaling complex (DISC), which recruits and activates caspase-8[54–56]. Activated caspase-8 then initiates apoptosis by cleaving and activating downstream executioner caspases, such as caspase-3 and caspase-7[57,58]. The death receptor pathway plays a critical role in immune surveillance and in the elimination of cells that are infected or damaged beyond repair. Dysregulation of this pathway is implicated in various diseases, including cancer, autoimmune disorders, and neurodegenerative diseases[46,59,60].

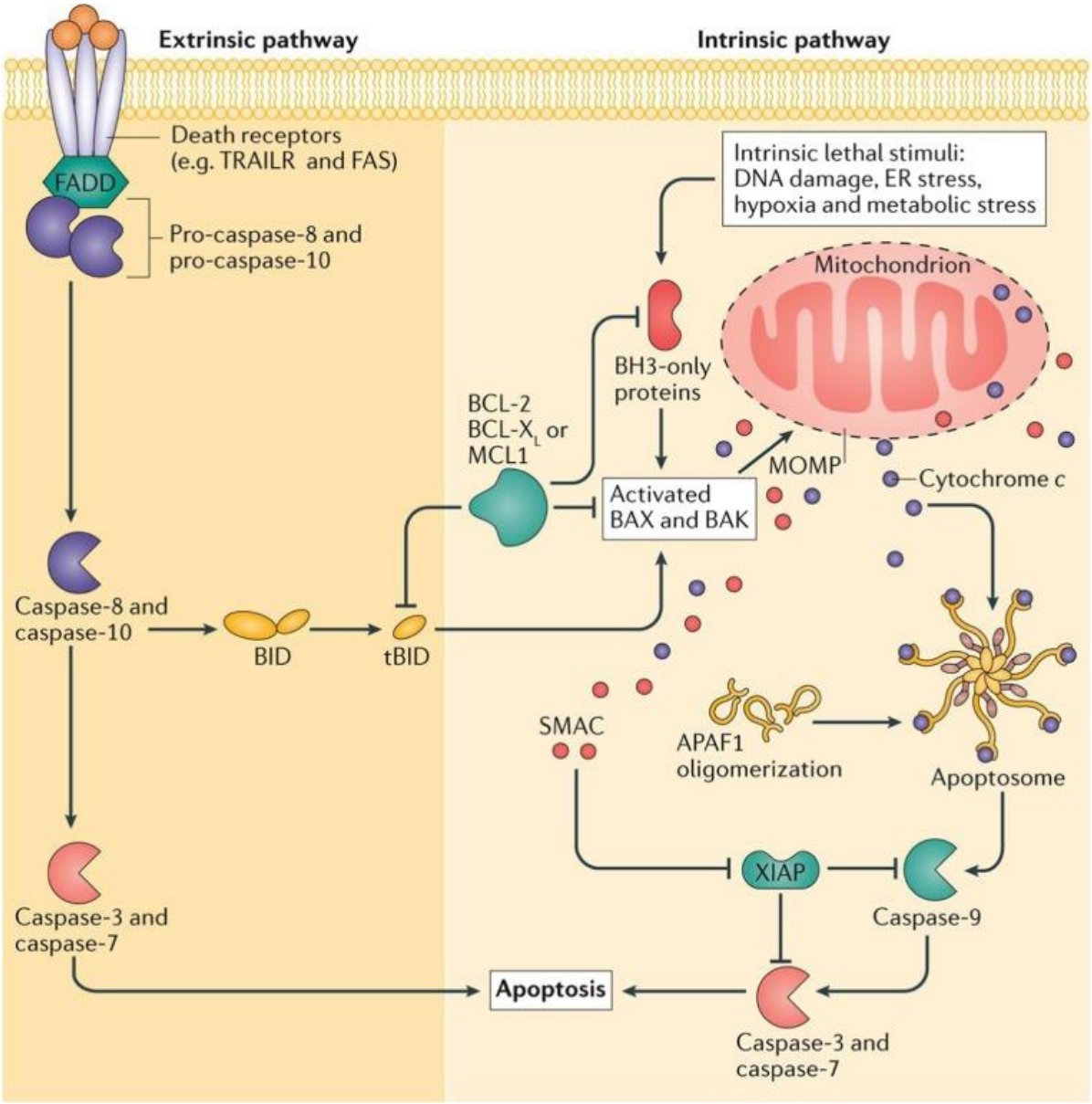

Fig.2: Overview of intrinsic and extrinsic pathways of apoptosis. *In the extrinsic apoptotic pathway, upon binding to their cognate ligand, death receptors such as tumor necrosis factor (TNF)-related apoptosis-inducing ligand (TRAIL) receptor (TRAILR) and FAS can activate initiator caspases-8 and 10 through dimerization mediated by adaptor proteins such as FAS-associated death domain protein (FADD). Active caspase-8 and caspase-10 then cleave and activate the effector caspase-3 and caspase-7, leading to apoptosis. The intrinsic pathway of apoptosis requires mitochondrial outer membrane permeabilization (MOMP). Cell stresses trigger Bcl-2 homology domain 3 (BH3)-only protein activation, leading to BAX and BAK activity that triggers MOMP. Anti-apoptotic Bcl-2 family proteins counteract this. Following MOMP, mitochondrial intermembrane space proteins such as second mitochondria-derived activator of caspases (SMAC) and cytochrome c are released into the cytosol. Cytochrome c interacts with apoptotic protease activating factor 1 (APAF1), triggering apoptosome assembly, which activates caspase-9. Active caspase-9, in turn, activates caspase-3 and caspase-7, leading to apoptosis. Mitochondrial release of SMAC facilitates apoptosis by blocking the caspase inhibitor X-linked inhibitor of apoptosis protein (XIAP). Caspase-8 cleavage of the BH3-only protein BH3-*

interacting death domain agonist (BID) enables crosstalk between the extrinsic and intrinsic apoptotic pathways. ER endoplasmic reticulum; MCL1 myeloid cell leukaemia 1; tBID truncated BID. From S.H. Suhaili, 2017, Biophys Rev[61].

3. Gasdermins in chronic inflammation

In recent years, gasdermins have emerged as potential players in the pathogenesis of COPD[62–64]. Specifically, the involvement of pyroptosis, and the roles of GSDMD in this context are at the forefront of chronic inflammation and lung diseases research[65–67]. The gasdermin family consists of five members: GSDMA, GSDMB, GSDMC, GSDMD, and GSDME. Among these, GSDMD and GSDME are the most prominently associated with pyroptosis (Fig.3) and, by extension, with COPD[68–70]. Accumulating evidence suggests that GSDMs are differently involved in the response to infection and cancers, implying complicated links between inflammation and pyroptosis and the development and progression of those diseases[71]. GSDMD is the most extensively studied gasdermin in the context of pyroptosis.

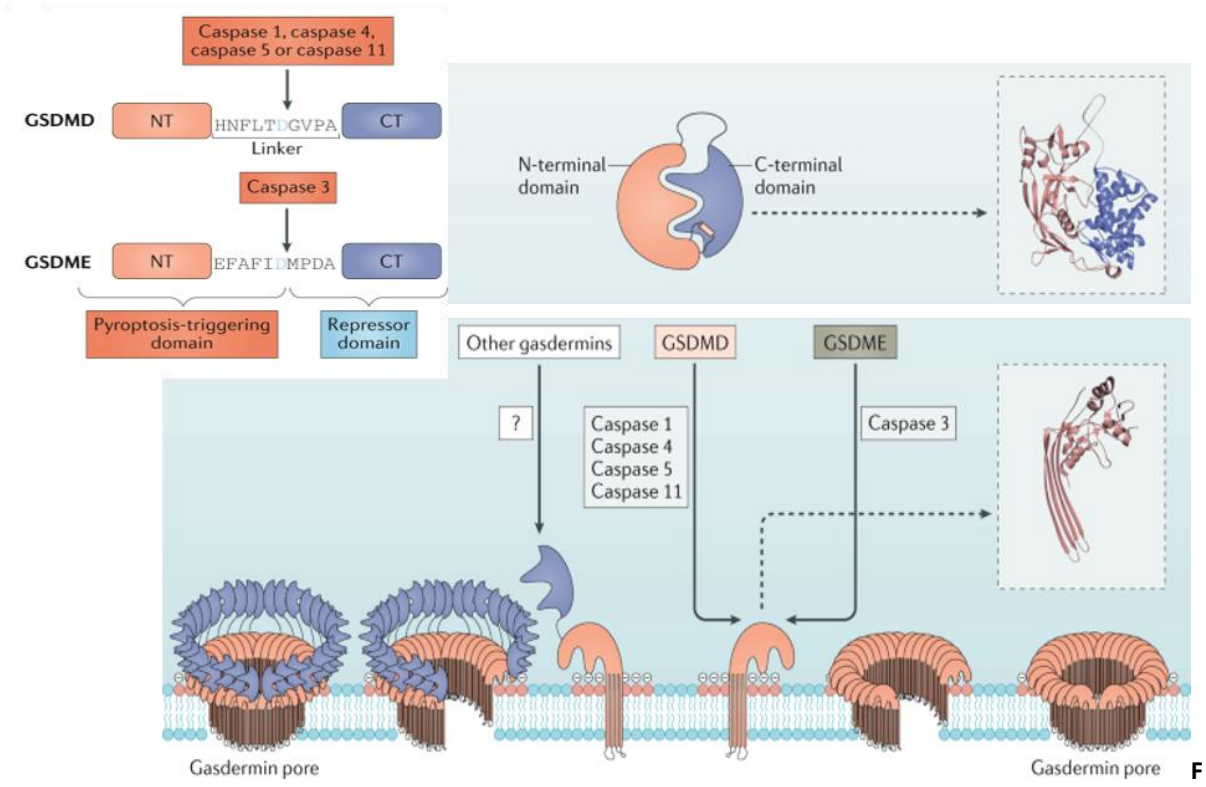

Fig.3: Mechanism of gasdermin membrane insertion and pore formation. *Active caspase interdomain interaction between the N-terminal gasdermin (GSDMNT) and C- terminal gasdermin (GSDMCT) domains keeps the protein in an autoinhibited state. Within the GSDMNT domain, helix α1 and a short β- hairpin located at the concave side of the β- sheet structure interact closely with the GSDMCT domain. In addition, a long loop stretches out from one end*

of the β- sheet to connect to GSDMCT. Once autoinhibition is disrupted, through mechanisms such as cleavage of gasdermin D (GSDMD) by mammalian caspase 1, mouse caspase 11 or human caspase 4/5 and GSDME, GSDMCT is released from the concave surface, thereby freeing GSDMNT for membrane insertion and pore formation. Membrane- targeting requires phospholipids with negatively charged head groups, as found on the inner leaflet of the plasma membrane. Compared with the autoinhibited state, the pore conformation of GSDMNT shows drastic conformational changes, involving the refolding of new β- strands that merge with the twisted β- sheet structure. These changes also generate new oligomerization interfaces that drive the assembly of a membrane- spanning β- barrel, the GSDMNT pore. From the structural perspective, gasdermin can be activated in the absence of interdomain cleavage by mechanisms that disrupt the intramolecular inhibition. From P. Broz, 2019, Nat Rev[72].

Upon inflammasome activation, inflammatory caspases, notably caspase-1, cleaves GSDMD. This cleavage event results in the formation of two GSDMD fragments: the N-terminal domain (GSDMD-NT) and the C-terminal domain (GSDMD-CT). GSDMD-NT is the critical mediator of pyroptotic cell death. It forms membrane pores in the plasma membrane, leading to the release of proinflammatory cytokines IL-1 and IL-18 as well as small DAMPs[73–76]. GSDMD was initially found to be expressed in the epithelial cells of the esophagus and stomach, and recent studies revealed that GSDMD is also highly expressed in other cell types, including fibroblasts[77,78]. A study published in 2022 found that cigarette smoke-induced gasdermin D activation in murine bronchoalveolar macrophages and bronchial epithelial cells dependently on NLRP3[79]. Liu et al. discussed the role of pyroptosis in respiratory diseases, including COPD. The study found that the NLRP3 inflammasome did not correlate with the severity of stable COPD patients, possibly due to the involvement of other inflammasomes[80]. Buscetta et al. investigated the mechanisms and consequences of gasdermin D activation in cigarette smoke-associated inflammation and lung disease. The study found that cigarette smoke promotes inflammasome-independent activation of caspase-1 and -4 leading to gasdermin D cleavage in human macrophages[81]. A 2023 study identified 26 COPD key genes, including gasdermins, using Weighted Gene Co-expression Network analysis (WGCNA)[82].

GSDME is another gasdermin family member, although its activation mechanisms differ from GSDMD. GSDME is activated downstream of caspase-3 [83]. It has been proposed that in specific cell types (such as tumor cells) GSDME may turn immunogenically silent apoptosis into pro-inflammatory pyroptotic death. Atan et al. in 2021, found that GSDME-mediated epithelial-cell pyroptosis is positively correlated with abnormal mucosal inflammation in Crohn's disease[84]. Another study published in 2020 found that GSDME correlates with mucosal inflammation in

inflammatory bowel disease (IBD) patients[85]. GSDME expression also positively correlated with the estimated infiltration value of tumor-associated fibroblasts for several types of cancer, including lung cancer[86]. This study suggests that GSDME may play a role in chronic inflammatory conditions. However, more research is needed to understand whether a relationship exists between GSDME and chronic inflammation in the context of COPD. Several studies provide evidence of gasdermins activity in structural cells such as epithelial and fibroblasts. A study published in 2023 found that GSDME expression was positively correlated with mitochondrial gene content, indicating that GSDME potentiates macrophage pyroptosis[87,88]. The study also found that GSDME ablation restrains macrophage migration and inflammation, suggesting that GSDME may play a role in inflammation in various cell types, including fibroblasts[89-90]. Of note, growing evidence suggests that there is an association between GSDMD and GSDME activation and fibrosis. Accordingly, several studies have shown that deletion of GSDME prevented the development of kidney fibrosis[91,92], and GSDMD plays a key role in scleroderma and bleomycin-induced skin fibrosis and silica-induced pulmonary fibrosis[93–95].

In summary, there is evidence to suggest that gasdermins are expressed in various cell types, including epithelial cells and fibroblasts, and play a role in regulation unconventional protein secretion, pyroptosis and inflammation. However, more research is needed to fully understand the mechanisms involved in gasdermins activity in structural cells such as epithelial and fibroblasts. Identifying whether key players of inflammasome-related pathways are involved in CS-associated inflammation and fibrosis has critical relevance for our understanding of disease pathogenesis and may lead to the discovery of new therapeutic targets for the development of new, more effective therapies[96]. The identification of gasdermin fragments, such as GSDMD-NT, in blood or sputum samples could serve as potential biomarkers for COPD. Elevated levels of these fragments may indicate the presence of ongoing pyroptotic cell death, offering insights into disease severity and progression. Biomarkers are crucial for early diagnosis and monitoring of COPD. While the connection between gasdermins and COPD is an exciting avenue of research, several questions remain unanswered. Further studies are required to elucidate the precise mechanisms of gasdermin activation in the context of COPD. It is still not entirely clear whether and how specific stimuli, such as cigarette smoke or

oxidative stress, lead to the activation of GSDMD and GSDME. Understanding the precise contribution of pyroptosis and gasdermins in this complex context is an ongoing challenge.

4. Fibroblasts in chronic inflammation

While the roles of immune cells and airway epithelium in COPD have been widely investigated during the past years [97–100], lung fibroblasts have emerged as critical players[101–104].

Traditionally regarded as essential contributors of tissue repair and extracellular matrix (ECM) homeostasis, lung fibroblasts have transitioned from the periphery of COPD research to a central focus. Their activities significantly contribute to the structural changes observed in COPD, including fibrosis and loss of lung elasticity.

In healthy lungs, the extracellular matrix is maintained by the activity of resident fibroblasts and represents a loose meshwork of collagens, elastin, and fibronectin anchored. The ECM components include fibrillar proteins such as collagen and fibronectin, which provide the tensile strength and elastic recoil necessary for normal lung function[105–108]. Collagen I (COL-I) is a major component of the lung ECM and contributes to the overarching architecture of the lung, while fibronectin is involved in providing structural support and promoting cell adhesion. Fibronectin is known to regulate many aspects of fibroblast biology[109,110]. It has been shown that TGF-β1 increases fibronectin expression in human lung fibroblasts, and this increased expression is associated with the fibrotic lung fibroblast phenotype.

Decorin, another ECM component, is a small leucine-rich proteoglycan that interacts with collagen and regulates fibrillogenesis, contributing to the structural integrity of the ECM. Decorin is an ECM proteoglycan that antagonizes TGFβ activity and inhibits its profibrotic biological activity. Recombinant expression of decorin in the lung airways of mice has been shown to inhibit bleomycin-induced pulmonary fibrosis[111].

Thrombospondin (TSP-1), a matricellular protein, is also present in the lung ECM and is known to play a role in tissue repair and fibrosis[112]. Matricellular proteins have regulatory roles and modulate cell-matrix interactions. Gene set enrichment analysis (GSEA) results indicated a positive association between TSP-1 expression and gene sets related to the reactive oxygen species (ROS) pathway in lung fibroblasts. TSP-1 overexpression alone induced mild

endoplasmic reticulum (ER) stress and pulmonary fibrosis, and it even exacerbated bleomycin-induced ER stress and pulmonary fibrosis[113].

Lung fibroblasts regulate the balance between matrix metalloproteinase (MMPs) and tissue inhibitor of metalloproteinase (TIMPs), which are essential for ECM turnover. An imbalance in this regulation can result in excessive ECM degradation or deposition, leading to structural abnormalities in COPD.

ADAMTS1 is a metalloproteinase that is involved in the processing of ECM proteins and has been implicated in tissue remodeling and repair. Recently Hu et al., found that ADAMTS1 was highly expressed in non-small cell lung cancer (NSCLC) tissues, which promoted cell proliferation, migration, invasion, and epithelial to mesenchymal transition (EMT) of NSCLC cells[114].

Lung fibroblasts' contributions extend beyond structural support and now encompass intricate interactions with immune cells, their ability to secrete pro-inflammatory mediators, and their involvement in ECM remodeling[115,116].

Lung fibroblasts actively participate in the chronic inflammation characteristic of COPD. They release pro-inflammatory cytokines, including IL-6, interleukin-8 (IL-8), and TNF. Moreover, fibroblasts secrete chemokines like CCL2, which attract immune cells to the site of inflammation, further amplifying the inflammatory cascade[117–120]. This reciprocal crosstalk creates a dynamic and complex immune microenvironment[117]. Various signaling pathways, including NF-κB and MAPK, play crucial roles in fibroblast-mediated inflammation[121,122]. In response to injury and inflammation, lung fibroblasts can differentiate into myofibroblasts expressing α-smooth muscle actin (α-SMA), contractile cells that produce ECM components[123]. This transition is implicated in the fibrotic changes observed in COPD and other lung diseases.

In a recent study increases in αSMA+ myofibroblasts were observed in subepithelial reticular basement membrane, lamina propria and adventitia in both the smoker and COPD groups compared to no-smoker controls. The increase in the myofibroblast population in the lamina propria was strongly associated with decrease in lung function, lamina propria thickening, increase in ECM protein deposition, and finally EMT activity in epithelial cells[124].

In cardiac fibroblasts, caspase-1 leads to the maturation of IL-1β, myofibroblast differentiation, and COL-I synthesis[125,126]. In SSc (Systemic sclerosis) primary dermal and lung fibroblasts Caspase-1 activation has been linked to TGF-1-mediated collagen expression, emphasizing its role in tissue remodeling and fibrosis[127].

In lung fibroblasts, inflammasome activation can occur in response to a variety of stimuli, such as infections, cellular stress, and inflammatory cytokines. Furthermore, the NLRP3 inflammasome is activated in human lung fibroblasts following treatments such as nigericin and paraquat [128129]. The activation of the NLRP3 inflammasome suggests an inflammatory response in lung fibroblasts triggered by these agents, which could be relevant to lung diseases and tissue damage. During viral infection, activation of the NLRP3 inflammasome by integrating multiple cellular and molecular signaling implicates robust inflammation, fibroblast proliferation, activation of myofibroblast, matrix deposition, and aberrant epithelial-mesenchymal function[130]. The non-canonical inflammasome pathway, involving NLRP3 and caspase-4, is implicated in IL-1β production in primary endometrial epithelial and stromal fibroblast cells[131]. Cancer-associated fibroblasts (CAFs) can sense DAMPs and activate the NLRP3 inflammasome pathway, resulting in pro-inflammatory signaling and IL-1β and IL-8 secretion[132,133]. The production of IL-1β and IL-18 by lung fibroblasts, following caspase-1 activation, can contribute to local inflammation in the lung.

Inflammatory signals can directly impact lung fibroblasts, driving their differentiation into myofibroblasts. This differentiation process is mediated by signaling pathways involving TGF-β, which activates caspases, particularly caspase-3[134]. Lung fibroblasts exposed to certain inflammatory signals or environmental factors can become sensitized to inflammasome activation and caspase-1 production[135,136]. CSE has profound effects on lung fibroblasts influencing their differentiation, function, and signaling pathways. CSE can influence the production and remodeling of the ECM by lung fibroblasts. This can disrupt the balance between ECM synthesis and degradation, contributing to tissue remodeling and fibrosis. Cigarette smoke can enhance the proliferation of lung fibroblasts, this hyperproliferative response can contribute to excessive ECM production and tissue remodeling. Exposure to cigarette smoke has been shown to have an impact on fibronectin release from human lung fibroblasts. A study demonstrated that cigarette smoke extract can directly upregulate fibronectin deposition from fibroblasts[137] notably, CSE promotes myofibroblast differentiation[138,139]. The specific relationship between cigarette smoke and inflammasome-related response in human lung fibroblasts has not been directly addressed in literature so far. Cigarette smoke exposure can influence the activation of caspases, particularly caspase-3, in lung fibroblasts. Caspase-3 activation is often associated with apoptosis, and its dysregulation

may lead to altered cell survival and tissue homeostasis. The exact role of caspases in lung fibroblasts in response to cigarette smoke is an area of ongoing research.

A study published in 2013 found that cigarette smoke activates caspase-3, the key regulatory point in apoptosis, in fetal rat lung fibroblast cells[140]. A review article published in 2023 discussed the role of apoptosis in the development of lung disease, including fibrosis. The article mentioned that increased apoptosis of alveolar epithelial cells and decreased apoptosis of fibroblasts may play an important role in the pathogenesis of disease. Blockade of caspase-3 has been shown to prevent alveolar epithelial cell apoptosis and pulmonary fibrosis [141].

On the other hand, cigarette smoke exposure has been linked to premature cellular senescence in various lung cell types, including fibroblasts. Cigarette smoke exposure induces cellular senescence in lung fibroblasts, which can lead to impaired lung repair and contribute to the pathogenesis of lung diseases [142,143]. CSE upregulates two pathways linked to cell senescence, p53 and p16-retinoblastoma protein pathways, it inhibits the proliferation of normal fibroblasts thus promoting cellular senescence, and inhibits alveolar repair[144,145].

Studies showed that CS leads also to increased oxidative stress is involved in the pathogenesis of lung diseases[146].

Cigarette smoke exposure leads to the generation of reactive oxygen species (ROS) and oxidative stress in the lung [147], which can trigger the activation and differentiation of lung fibroblasts into myofibroblasts, thereby contributing to tissue remodeling and fibrosis.

In 2022 Zhang et al. described that cigarette smoke exposure can activate lung fibroblasts by inducing redox imbalance and mitochondrial oxidative stress, which contributes to pulmonary fibrosis[148]. The specific relationship between cigarette smoke, decorin and ADAMTS1 in human lung fibroblasts is not explicitly addressed in the search results.

Overall, all these findings highlight the complex interplay between cigarette smoke and cellular responses in lung fibroblasts and suggest that multiple pathways participate in CS-associated inflammatory responses in lung fibroblasts.

Further research is needed to fully understand the mechanisms involved in cigarette smoke-induced activation of lung fibroblasts and their contribution to lung diseases.

Aims of the project

There is limited information available in the current literature on the involvement of the NLRP3 inflammasome in human lung fibroblasts that are exposed to cigarette smoke. The activation of the inflammasome and its subsequent effects upon exposure to cigarette smoke is still under investigation. It is not yet fully understood if caspases and gasdermins contribute to fibroblast activation when exposed to cigarette smoke. This PhD project aims to address this gap in knowledge by focusing on the following objectives:

1. **Investigate the NLRP3 inflammasome activation and downstream responses in human lung fibroblasts exposed to cigarette smoke extracts:**

This aim will be pursued through the exploration of the cellular responses of MRC5, human lung fibroblasts cell line, exposed to cigarette smoke. Unraveling whether inflammasomes participate to cigarette smoke-induced fibroblast activation holds the potential to provide crucial insights into the molecular mechanisms contributing to smoke-related lung diseases.

2. **Validate key findings in primary human lung fibroblasts (phLFs):**

The validation of key findings from the MRC5 cell line on patient-derived human lung fibroblasts is essential to ensure the relevance and translational potential of the research. While the MRC5 cell line, derived from human embryonic lung fibroblasts, is a valuable model for studying cellular responses, including those related to fibroblast activation and inflammation, it is crucial to confirm these findings in phLFs to establish the clinical significance and applicability of the results. This step is important due to the unique characteristics of phLFs, such as their specific gene expression profiles and functional properties. Therefore, selected key findings of the previous aim will be validated in phLFs. During the six months of the research period at the University Medical Centre of Groningen N=10 phLFs from a collection of Professor Corry-Anke Brandsma will be used. At this point it is clear that the establishment of a collection of primary human lung fibroblasts directly isolated from lung tissue is necessary for this validation process, to this purpose once back to the RiMed laboratories in Palermo, the project aims to start a collection of phLFs.

3. **Evaluate cleaved GSDMD and caspase-3 in lung tissue sections:**

The third objective involves the assessment of cleaved Gasdermin D and cleaved caspase-3 in lung tissue sections using immunohistochemistry. These proteins are crucial in cell death and inflammation processes. By employing this technique, the aim is to identify and quantify cell death and inflammatory responses within lung tissue, bridging the gap between cellular studies and the actual tissue context. Within the Cost Action Mye-InfoBank CA20117 we proposed to test the hypothesis of a role for cleaved GSDMD as a biomarker of chronic inflammation. This hypothesis is currently under evaluation as part of the COST project. The potential implications of this hypothesis extend to the fields of chronic inflammation and cancer, particularly in the context of lung and colorectal cancer. The ongoing evaluation of GSDMD as a biomarker of chronic inflammation represents a significant step in understanding its potential role in disease progression and its utility as a therapeutic target.

In summary, these planned tasks collectively constitute a research strategy aimed at deepening our understanding of the molecular responses of human lung fibroblasts to cigarette smoke exposure. The overarching goal is to generate insights into how smoking influences lung health, potentially leading to the development of therapeutic strategies or preventive measures for smoke-related lung diseases such as chronic obstructive pulmonary disease. The anticipated outcome of this research is a more profound comprehension of the underlined mechanisms.

Materials and methods

1. Cell culture

1.1. MRC-5 cell line

The MRC-5 cell line is a widely used cell line in biomedical research. It was derived from the lung tissues of a 14-week-old male fetus in 1966. MRC-5 cells are a diploid cell line, meaning they contain two sets of chromosomes, and they have a relatively long lifespan compared to other cell lines. These cells are commonly used in virology, vaccine development, and drug testing. The MRC-5 cell line is particularly useful for studying respiratory viruses, as it is derived from lung tissue. It has been instrumental in advancing our understanding of various diseases and has contributed to the development of numerous medical treatments. The used culturing methods follow. One cryotube was transferred from liquid nitrogen into 37°C bath, to rapidly

thaw the cells. Cells were transferred directly into a T25 flask with 5ml of pre-warmed EMEM medium supplemented with 1x Penicillin/Streptomycin (P/S), 1x L-glutamine, HEPES 10mM, Sodium pyruvate 1mM, 10% Fetal bovine serum (FBS), all reagents were from Euroclone, Milan, Italy.

The flask was incubated and cell medium was refreshed one time a week. When cells arrived at 80-90% of confluence, were detached and 1.000.000 cells were transferred into T75 flask. The flask was incubated and cell medium was refreshed one time a week. When cells arrived at 80-90% of confluence, were detached and 4.000.000 cells were transferred into T175 flask. For the experiments, 250.000 cells/well were seeded into 6-well plate, and 10.000 cells/well were seeded into 96-well plate.

1.2. Patients derived human lung fibroblasts (phLFs)

1.2.1. Isolation from lung resections

During my research period in the Department of Pathology and Medical Biology at the Medical University of Groningen, Netherlands, I worked with a collection of primary lung fibroblasts and peripheral lung tissue from subjects undergoing lung transplantation or tumor resection surgery. Resected lung tissue was isolated from an area distal from the tumor and that was macroscopically and histologically normal. Primary parenchymal lung fibroblasts were isolated as described before[149]. Patients' characteristics are shown in Table T1.

For the collection at RiMed laboratories, fresh lung tissue samples were obtained from patients undergoing surgery for lung cancer (areas well distant from the tumor were used for this study). The study was conducted in collaboration with ISMETT IRCCS (the study protocol was approved by the Institutional Review Board for human studies at IRCCS ISMETT, # IRRB/19/19). Patients' characteristics are shown in table T2. For the isolation of phLFs the resection was washed filling 50ml falcon tubes with 10ml PBS + Pen/Strept 1X (100uM) and shacked vigorously to properly clean the sample. This step was repeated at least 4 times, the final wash discard should be transparent. The sample was cut in small pieces using a sterile scalpel. Each piece was rubbed into 100mm treated petri dishes. 3ml of HAMF12 (Lonza LOBE12615F) supplemented with amphotericin, P/S (1x, Euroclone, Milan, Italy) and FBS 10% (called complete medium) was added and dishes were incubated at 37°C. Every 48h the medium was changed and was checked for contamination. When confluency was 80-90%, cells were

detached using Trypsin-EDTA 1x in PBS (Euroclone, Milan, Italy), centrifugated at 180 rfc 5 minutes RT and 800.000 cells per vial were frozen using HAMF12 complete medium supplemented with 1% DMSO and FBS 50%.

1.2.2. Culturing

To proceed with the experiments one cryotube was transferred from liquid nitrogen into 37°C bath, to rapidly thaw the cells. Cells were transferred directly into a T25 flask with 5ml of pre-warmed HAMF12 complete medium. When cells arrived at 80-90% of confluence, were detached and were transferred into 5 T25 flasks. After one-week cells reached 80-90% confluence and were used for the experiments. 100.000 cells/well were seeded into 12-wells plate.

2. Flow Cytometry

Before plating the experiments, cells were characterized by flow cytometry using two different antibodies. Cells were washed with PBS, then centrifuged for 5 minutes RT, and stained for 10 minutes RT in darkness with 1µl of fluorescent-tagged antibody specific for CD90-PE (130-114-860, Miltenyi Biotech) and EPCAM-APC (130-111-000, Miltenyi Biotech). CD90 is a small membrane glycophosphatidylinositol (GPI) anchored protein, it is highly expressed in fibroblasts and therefore was selected as positive marker and EPCAM cell adhesion molecule, highly expressed in epithelial cells. After staining, cells were washed with PBS then analyzed by flow cytometry using CytoFLEX (Beckman Coulter, Brea, CA).

3. Immunohistochemistry on FFPE of lung tissue samples

Lung tissue samples were obtained from patients undergoing surgery for lung cancer. Sampling did not interfere with the subsequent examinations of the specimens by the pathologist. The study protocol was approved by the Institutional Review Board for human studies at IRCCS ISMETT (IRRB/19/19) and conducted by the Declaration of Helsinki. Informed written consent was obtained from each patient.

To study Cleaved-GSDMD, the patients were grouped as follows: never smoking patients (no-smokers, n = 3); patients who had stopped smoking from more than 2 years (ex-smokers, n = 5); and smoker patients (>15 pack/year) (smokers, n = 6).

To study cleaved caspase-3, the patients were grouped as follows: never smoking patients (No-Smokers, N = 6); smoker patients (>15 pack/year) (Smokers, N = 5). Characteristics of patients are reported in Table T2-T3. The presence of COPD patients in selected groups was excluded by performing spirometry evaluation. COPD patients were classified based on GOLD Guidelines 2019 (https://goldcopd.org/pocketguidereferences/gold-2019-pocket-guide-references/): Forced expiratory volume in one second (FEV1) less than 80% of reference, FEV1/Forced Vital capacity (FVC) less than 70%, and bronchodilatation effect less than 12%. All recruited subjects had negative skin tests for common aeroallergen extracts and had no history of asthma and/or allergic rhinitis. The patients were not under corticosteroid therapy (inhaled or systemic) and were not under antibiotics. Patients did not have exacerbations during the month preceding the study.

For immunohistochemistry (IHC), 5-µm formalin-fixed and paraffin-embedded peripheral lung sections were deparaffinized in xylene and rehydrated through a series of graded alcohol. The sections were initially treated at 75°C in sodium citrate (pH 6.5) for antigen retrieval. After being washed, the sections were incubated with the primary antibody specific for cleaved GSDMD (36425S Cell Signaling Technologies, 1:500) and for cleaved caspase-3 (9661S Cell Signaling Technologies, 1:500) at 4 °C overnight. Immunoreactivity was visualized using a Mouse and Rabbit Specific HRP/DAB Detection IHC kit (ab64264, Abcam, USA) according to the manufacturer's instructions and counterstained with Mayer's Hematoxylin for 45 s. Finally, the slides were prepared for observation with coverslips, using a permanent mounting medium (Vecta Mount, Vector, H-5000). The sections were observed with an optical microscope (Microscope Axioscope 5/7 KMAT, Carl Zeiss, Milan, Italy) connected to a digital camera (Microscopy Camera Axiocam 208 color, Carl Zeiss, Milan, Italy) for evaluation. Two independent observers (F.B. and F.R.) evaluated the reactions on two separate occasions and performed an immunomorphological evaluation to distinguish and characterized the cleaved GSDMD/cleaved caspase-3 positive cells. A quantitative analysis to determine the percentage of immunopositivity was also carried out. All evaluations were made at a magnification of 400× and the percentage of positive cells was calculated in a high-power field (HPF) and repeated for 10 HPFs. The arithmetic mean of counts was used for statistical analysis.

4. Cigarette smoke extract

Cigarette smoke extract (CSE) was prepared using the 3R4F reference cigarettes (The Tobacco Research Institute, University of Kentucky[9,150,151]). Briefly, one cigarette was smoked using a peristaltic pump set at 70 rpm for 5 minutes in 10ml of PBS to generate a CSE solution. The CSE solution was filter-sterilized through a 0.22µm pore filter and used within 20 minutes. The CSE optical density (OD) was evaluated spectrophotometrically at a wavelength of 260nm. A solution with OD=1 was considered 100% CSE. For MRC-5 an phLFs stimulation, CSE was diluted into respectively EMEM 1%FBS and HAMF12 1%FBS. Solutions at 5- 10- 20% CSE were used.

5. LDH assay

CytoTox 96® Non-Radioactive Cytotoxicity Assay (G1780, Promega, Madison, Wisconsin, United States) is a colorimetric test that measure the release of lactate dehydrogenase (LDH), a stable cytosolic enzyme released upon cell lysis, in the supernatant of cells.
This kit measures the conversion of a tetrazolium salt into a red formazan product, and the amount of colour formed is proportional to the number of lysed/dead cells.
When cells reached 80-90% of confluence were stimulated with 5-10-20% CSE for 72h at 37°C and 5% of CO2. At the end of the experiment, 50µl of supernatants were transferred into a new 96-well plate, then 50µl of CytoTox 96 Non-Radioactive Cytotoxicity Assay was added to each well and the plate was incubated at room temperature for 30 minutes in darkness. After 30 minutes, 50µl of stop solutions were added into each well, and the absorbance signal was read at 490nm using Spark-Tecan plate reader.

6. MTS

The CellTiter 96® AQueous One Solution Cell Proliferation Assay is a colorimetric assay used for monitoring cell viability. When cells reached 80-90% of confluence were stimulated with 5-10-20% CSE for 72h at 37°C and 5% of CO2. At the end of the experiment, 20ul of CellTiter reagent

were added directly into each well and the plate was incubated at 37°C and 5% of CO2 for 20'. The absorbance was read at 490nm by using the Spark-Tecan plate reader. The quantity of formazan produced by cells is directly proportional to the number of living cells, data expressed in absorbance 490nm.

7. Caspase activity assay

The extracellular activity of caspase-1 caspase-8 and -3/7 was determined using respectively CaspaseGlo 1 -8 and -3/7 homogeneous luminescent assay kits (Cat# G9951, Cat# G8202, Cat# G8093, Promega Corporation, Madison, Wisconsin, USA), following the manufacturers' instruction [152]. This is a homogeneous bioluminescent method that directly measures the activity of caspases in cell supernatants.

When cells reached 80-90% of confluence were stimulated with 5% and 10% CSE for 72h. MRC-5 cells were treated 1h prior of CSE stimulation with the following: MCC950 (NLRP3 inhibitor, Sigma-AldrichCP, 456773, 10µM), z-IETD-fmk (Caspase-8 inhibitor, Sigma-Aldrich, 218759, 0.1 µM); or simultaneously with N-acetyl cysteine (NAC, antioxidant and cytoprotectant, Sigma-Aldrich, A9165, 600µM) for 72h at 37°C and 5% of CO2.

phLFs were treated 1h prior of CSE stimulation with z-IETD-fmk (caspase-8 inhibitor, 0.1 µM), z-VAD (pan caspase inhibitor, 100µM); or simultaneously with N-acetyl cysteine (NAC, antioxidant and cytoprotectant, 600µM) for 72h at 37°C and 5% of CO2.

At the end of the experiment, 50µl of supernatants were transferred into a new 96-well plate and 50µl of CaspaseGlo reagent was added. Then the plate was incubated for 1h at room temperature in the dark. Next, the luminescence was measured by using the GLOMAX microplate reader GM3000, and the results in Relative Luminescence Units (RLU) were plotted into a graph.

8. Western Blot

When cells reached 80-90% of confluence were stimulated with 5% and 10% CSE for 72h. Cells were treated 1h prior of CSE stimulation with z-IETD-fmk or simultaneously with NAC for 72h at 37°C and 5% of CO2.

At the end of the experiment MRC-5 cells were lysed using a lysis buffer (10 mM Tris–HCl, 50 mM NaCl, 5 mM EDTA, 1% Nonidet P-40), protease inhibitor (P8340, Sigma-Aldrich, St. Louis, MO), and phosphatase inhibitor (P0044, Sigma-Aldrich).

PhLFs were lysed using RIPA buffer (Pierce, 89900), protease inhibitor (P8340, Sigma-Aldrich, St. Louis, MO), and phosphatase inhibitor (P0044, Sigma-Aldrich). The total protein content was determined using the Bradford protein assay kit (Thermo Fisher, Waltham, MA). A total of 50µg protein was loaded and resolved by SDS-PAGE (3450124, Gel Precast Criterion XT 4-12%) (Bio-Rad, Hercules, CA) and blotted onto nitrocellulose membranes (Bio-Rad, Hercules, CA). Membrane was incubated overnight with the following primary antibodies:

Recombinant Anti-DFNA5/GSDME antibody- N-terminal (ab215191, abcam); cleaved caspase-3 (9661S Cell signalling); NLRP3 (15101S) from Cell Signalling (Danvers, Massachusetts, United States); Gasdermin D Full-Length (NBP2-33422) from Novus Biologicals (St. Louis, Missouri); IL-1beta (af-201-na) from R&D (Minneapolis, Minnesota, United Stated); anti-caspase-1 (AG-20B-0048-C100) from Adipogen (San Diego, USA); recombinant anti-IL-18 (ab207324) from Abcam (Cambridge, United Kingdom) and ASC (sc-271054) from Santa Cruz Biotechnology (Santa Cruz, California, United States). All the antibodies were used at 1:500 and incubated at 4C° over night. As loading control, β-actin was detected (sc-81178, from Santa Cruz Biotechnology 1:10.000).

The LiCOR secondary antibodies were used as reported: goat-anti-mouse from LiCOR IRdye 800CW (926-32210, Lincoln, NE, USA) at 1:5000, donkey-anti-rabbit from LiCOR IRDye 680RD (926-68071) at 1:5000 and donkey-anti-goat from LiCOR IRDye 680RD (926-68074) at 1:5000.

The blots were analysed using the Odyssey Imaging System (LI-COR, Lincoln, NE).

9. ELISA

When cells reached 80-90% of confluence were stimulated with 5% and 10% CSE for 72h. Cells were treated 1h prior of CSE stimulation with z-IETD-fmk or simultaneously with NAC for 72h at 37°C and 5% of CO2. At the end of experiments cells supernatants were collected and centrifuged for 5 minutes at 500g at 4°C before storing them at -20°C.

The following ELISA kits from R&D Systems, Minneapolis, MN were used following manufacturer instructions: ProCollagen-I DY6220, Fibronectin DY1918, IL-1β DY201, IL-18

DY318, IL-6 DY206, IL-8 DY208, ADAMTS-1 DY2197, TSP1 DY3075, Decorin DY143 and DuoSet ancillary reagent kit DY008.

To calculate the results, a standard curve was constructed by plotting the mean absorbance, for each standard, on the y-axis, while the concentration was plotted in x- axis. The concentration of each sample was obtained through the interpolation of the absorbance (Abs) (calculated as the difference between the Abs at 450nm minus the Abs at 540nm) of each sample with the standard curve. Results are expressed in ng.

10. RT-q-PCR

When MRC-5 cells reached 80-90% of confluence were stimulated with 5% and 10% CSE for 72h. Cells were treated 1h prior of CSE stimulation with z-IETD-fmk or simultaneously with NAC for 72h at 37°C and 5% of CO2.

Total RNA was extracted using 1ml/well of TRIzol Reagent (Invitrogen, Waltham, Massachusetts, United States) to homogenize cell membranes. The TRIzol solution was transferred into a 1.5ml tube. In this passage it is possible decide to store the RNA at -80°C, or continue with the RNA extraction protocol.

The tube with TRIzol was incubated for 5 minutes at room temperature, then 200µl of chloroform was added and the tubes were shaken to separate the protein phase from the RNA phase. The tubes were incubated for 3 minutes at room temperature and then they were centrifuged for 15 minutes at 12000g at 4°C.

The aqueous phase (about 500µl), containing RNA, was transferred into a new tube, and 500µl of isopropanol were added. The tubes were incubated for 10 min at room temperature and then centrifuged for 10 min at 12000g at 4°C.

The supernatant was removed and the pellet (containing RNA) was washed with 1ml of 75% ethanol, and the tubes were centrifuged for 7 min at 7500g for 5 min at 4°C.

The ethanol was removed and RNA was left to dry on ice. When RNA was completely dry, the RNA was re-suspended in distilled water and total RNA was dosed by using the Tecan Nano-quant. Absorbance (Abs) at 260nm was measured and the concentration of RNA was calculated by using this following formula: Concentration of RNA [ng/(µl)]=Abs at 260nm*40*100

To evaluate the gene expression of NLRP3, IL-1β, IL-18 and GSDMD/E, the equivalent volume of 1µg RNA was reverse-transcribed to cDNA, using iScript cDNA Synthesis kit (Bio-Rad, Hercules, CA, USA). For each sample 4µl of 5x iScript Reaction Mix and 1µl of iScript Reverse Transcriptase (both supplemented into the kit) were added into the PCR tubes. Then the volume of each sample was adjusted by adding milliQ water up to 20µl. Then, the following protocol was used to do the retro-transcription (RT): Priming for 5 minutes at 25°C - Reverse transcription for 20 minutes at 46°C - RT activation for 1 minute at 95°C - bring the reaction back to 4°C. At the end of the protocol, 70µl of milliQ water were added for each tube to obtain a final concentration of 1µg/90µl.

Real-time quantitative polymerase chain reaction (real-time qPCR) was carried out on Step One Plus Real-time PCR System (Applied Biosystems, Waltham, Massachusetts, United States) using specific FAM-labelled probe and primers (pre-validated TaqMan Gene expression assay).

100 ng/µl of cDNA were amplified and for each sample 10µl of TaqMan Master Mix and 1µl of primer were added, then the volume of each tube was adjusted by adding milliQ water up to 20µl. Then, the following protocol was used to doing the real-time qPCR: 50°C for 2 minutes 95°C for 10 minutes - 40 cycles at 95°C for 15 minutes - 40 cycles at 60°C for 1 minutes.

The following primers from Applied Biosystems were used: NLRP3 (Hs00918082-m1), IL-1β (Hs01555410-m1), IL-18 (Hs01038788-m1) gasdermin-E (Hs00903185_m1) and gasdermin-D (HS00986739_g1).

Gene expression was normalized to GAPDH (Hs03929097g1) used as endogenous control gene. Relative quantification of mRNA was carried out with the comparative CT method ($2^{-\Delta CT}$) and was plotted as a relative fold-change graph.

11. Mitosox

MitoSox Red assay, live cells imaging technique was performed 72h after CSE stimulation.

The MitoSox Red assay is a widely used method for the selective detection of mitochondrial superoxide in live cells. The assay involves the use of a live-cell permeant dye, MitoSox Red, which rapidly and selectively targets the mitochondria. Once inside the mitochondria, MitoSox Red is oxidized by superoxide, resulting in a red fluorescence that can be detected and quantified using various techniques, such as fluorescence microscopy and flow cytometry. The

assay provides a valuable tool for studying mitochondrial superoxide production and its role in oxidative stress-related processes, as well as for investigating the impact of various experimental conditions, such as smoking, on mitochondrial function and redox signaling.
MRC-5 were treated with 5% and 10% CSE in the presence or not of NAC 600 µM; Rotenone 10µM was added for 24h as positive control. Confocal microscope Operetta CLS-Perkin Elmer was used to take and analyze the images at magnification 40x.

12. Immunostaining

The immunofluorescence (IF) assay was conducted. The assay involved the stimulation of MRC-5 cells for 72 hours with 10% cigarette smoke extract. Subsequently, immunofluorescence staining of alpha-smooth muscle actin, collagen I, and fibronectin antibodies was performed on the MRC-5 cells. The staining was carried out using specific dilutions of the antibodies, including 1:200 for COL I (SC-293182, Santa Cruz) and 1:500 for fibronectin (SC-514601, Santa Cruz) and α-SMA (MA5-11547, Invitrogen). The images were captured and analyzed using an Operetta CLS-Perkin Elmer microscope at a magnification of 40x. The IF assay allowed for the visualization and quantification of the expression and localization of the target proteins (α-SMA, COL I, and fibronectin) in the MRC-5 cells following CSE stimulation.

13. SA-β-gal staining

N=10 phLFs were exposed to 5%, 10% CSE and N=9 were exposed to paraquat (PQ, 100µM 24h), 1h before CSE or PQ stimulation cells were treated with 0.1µM of zIETD. After 72h cells cellular senescence was assessed with standard SA-β-gal staining. Fibroblasts were fixed with 2% formaldehyde + 0.2% glutaraldehyde in PBS for 5 min. After fixation, cells were incubated with the described staining solution (SA-β-gal detection 5-bromo-4-chloro-3-indolyl β-D-galactopyranoside (X-gal)) for 18 h (in a dry incubator) at 37°C. After incubation, the staining solution was washed away and nuclei were stained using ematoxylin. Four random images of every well with cells were taken using Zeiss AxioObserver Z1, Tissue Fax scanner objective Zeiss- LD "Plan-Neofluar" 20x/0,4 Corr Dry, Ph2 at a total magnification of ×200. SA-β-gal-

positive cells and total cells were scored blindly to calculate the percentage of SA-β-gal-positive cells.

14. Statistical analysis

Statistical analysis for MRC-5 was performed using the GraphPad Prism 9 software. Unless otherwise stated, data were expressed as mean ± SEM. Differences were identified using one-way repeated measures ANOVA with Bonferroni post hoc test. Differences with $p < .05$ were considered significant.

Statistical analysis for phLFs was performed using the GraphPad Prism 9 software differences were identified using the Wilcoxon test. Differences with $p<0.05$ were considered significant. Regarding sample size of human lung tissues, all available samples provided by the hospital were used. Unless otherwise stated, data were expressed as mean ± SEM. Differences were identified using one-way repeated measures ANOVA and Tukey's post hoc multiple comparisons test. The equality of group variances has been tested with Brown-Forsythe test. Differences with $p < 0.05$ were considered significant.

Results

1. Investigate the NLRP3 inflammasome activation and downstream responses in human lung fibroblasts exposed to cigarette smoke extracts (MRC-5, cell line)

1.1. Cigarette smoke induced activation of caspases

Viability was evaluated by MTS and LDH assays. Results showed that 5% CSE did not induce cell death. MRC-5 exposed to 10% CSE displayed some mortality although the increase in LDH release did not reach statistical significance (Fig.4A). The MTS assay showed that after stimulation with 10% CSE, cell viability decreased compared to the control condition (Fig.4A). Activation of caspase-1, -8, and -3/7 in response to 10% CSE in MRC-5 cell line was evaluated, we did not use 20% due to the high variability of the results obtained with LDH assay and the

higher mortality rates (Fig.4A). Cells were treated with CSE at 10% for 72h. CSE induced a dose-dependent increase of caspase-1, -8 and -3/7 activity (Fig.4B).

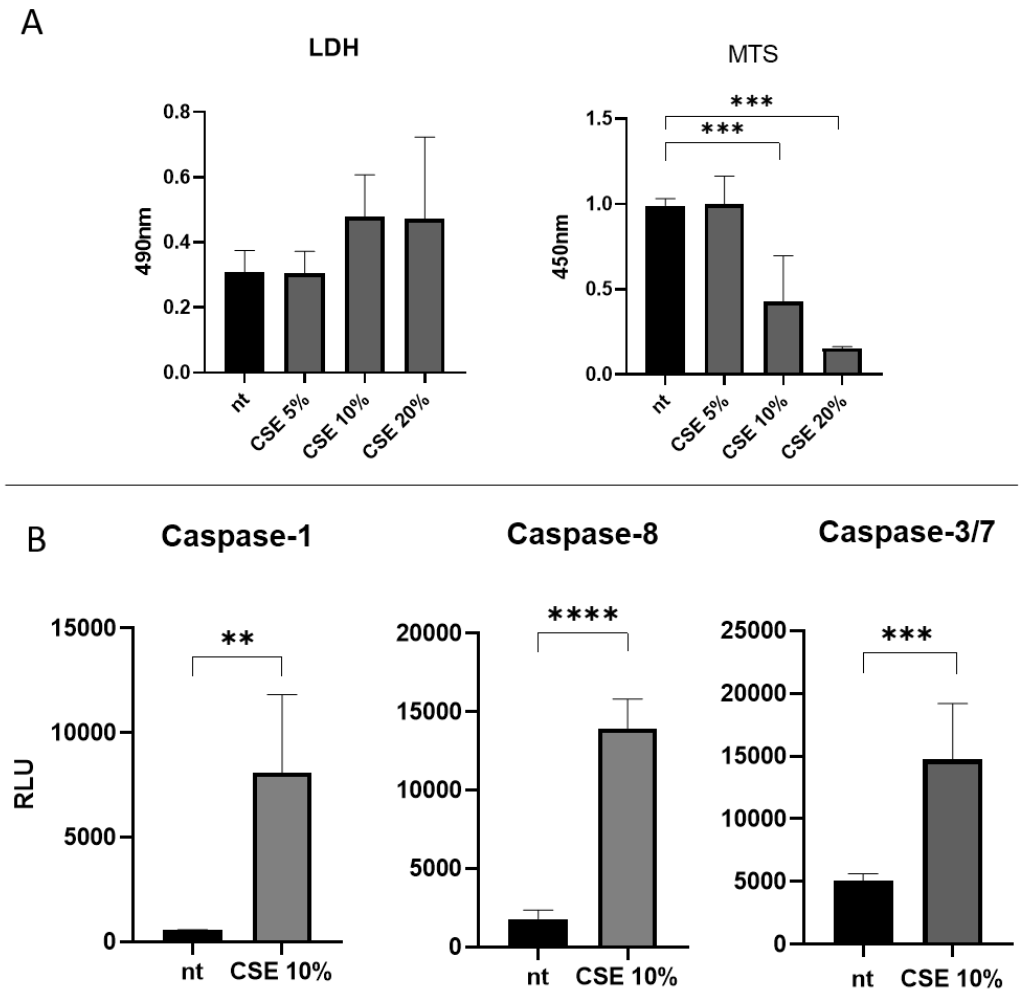

Fig.4: Impact of CSE on caspases activity and cell death. *MRC-5 cells were stimulated with the indicated concentration of CSE.* ***A.*** *LDH and MTS assays were run after 72h stimulation.* ***B.*** *The extracellular activity of caspase-1, caspase-8 and caspase-3/7 was investigated using an enzymatic assay. nt, no-treated. For each experiment 3 technical replicates were performed.*

Caspase-1 is activated by the NLRP3 inflammasome and other inflammasomes in many cellular types[29] . Buscetta et al. described that in human macrophages exposed to CSE Caspase-1 is activated independent of NLRP3 via the TLR4-TRIF-caspase-8 axis [38] . To investigate the mechanisms leading to activation of Caspase-1, the selective inhibitor of NLRP3, MCC950 and the caspase-8 inhibitor Z-IETD-fmk were added prior to CSE stimulation and caspase-1 activity was evaluated. Results showed that caspase-1 activation was independent of NLRP3 and caspase-8 (Fig.5A). Activated caspase-8 can cleave and activate downstream executioner

caspases, such as caspase-3 and caspase-7[57,58]. To investigate the caspase-3/7 activation by caspase-8, the selective inhibitor of caspase-8 Z-IETD-fmk was added before CSE stimulation and caspase-3/7 activity was evaluated. CSE-induced activation of caspase-3/7 was inhibited by the caspase-8 inhibitor zIETD (Fig.5C). Excessive ROS production can lead to the release of pro-apoptotic proteins, such as cytochrome c, triggering caspase activation[153,154] . To test the hypothesis that activation of caspase-1-8-3/7 was induced as response to oxidative stress, before CSE stimulation, we treated the cells with the cysteine prodrug N-acetyl cysteine (NAC), widely used as a pharmacological antioxidant and cytoprotectant[155]. As reported in Fig.5 (A, B, C) treatment with NAC inhibited the activation of caspase-1-8-3/7.

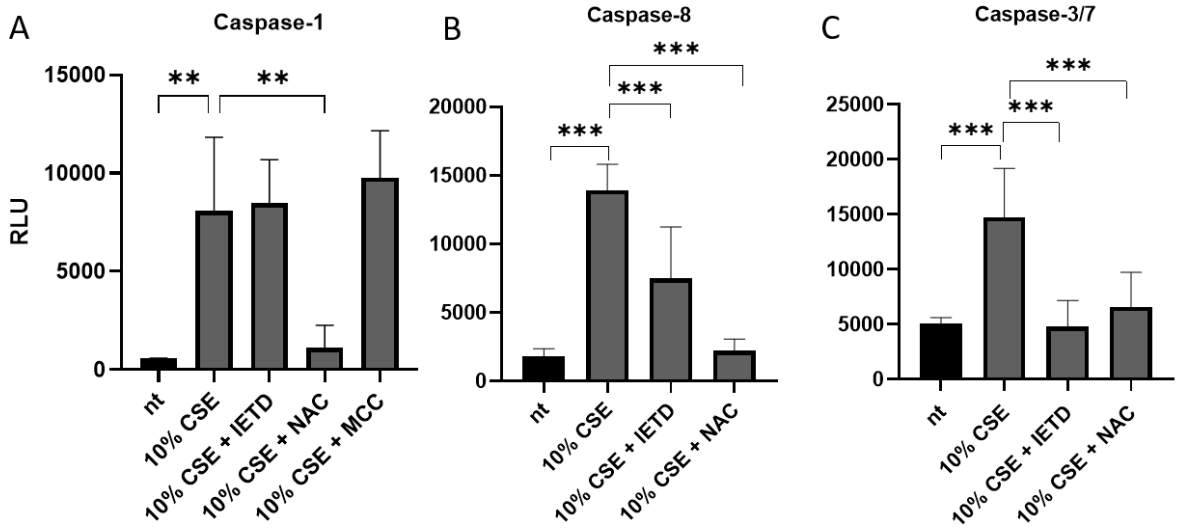

Fig.5: **Caspases activation mechanisms.** *MRC-5 cells were stimulated with CSE for 72h. MRC-5 cells were stimulated with 1µM MCC950, 0.1 µM z-IETD-fmk, 1h prior of stimulation with CSE. The antioxidant NAC was added at 500 µM simultaneously to the CSE. The extracellular activity of **A**. Caspase-1 **B**. Caspase-8 **C**. Caspase-3/7 was investigated using an enzymatic assay. For each experiment 3 technical replicates were performed. nt, no-treated.*

To confirm that NAC was effective at reducing oxidative stress we evaluated the production of mitochondrial superoxide (mSOX) in response to CSE with or without NAC. Cells were stained with the fluorescent probe MitoSox red and fluorescence was measured by Confocal microscope Operetta CLS-Perkin Elmer. CSE induced mSOX production while NAC inhibited mSOX generation (Fig.6).

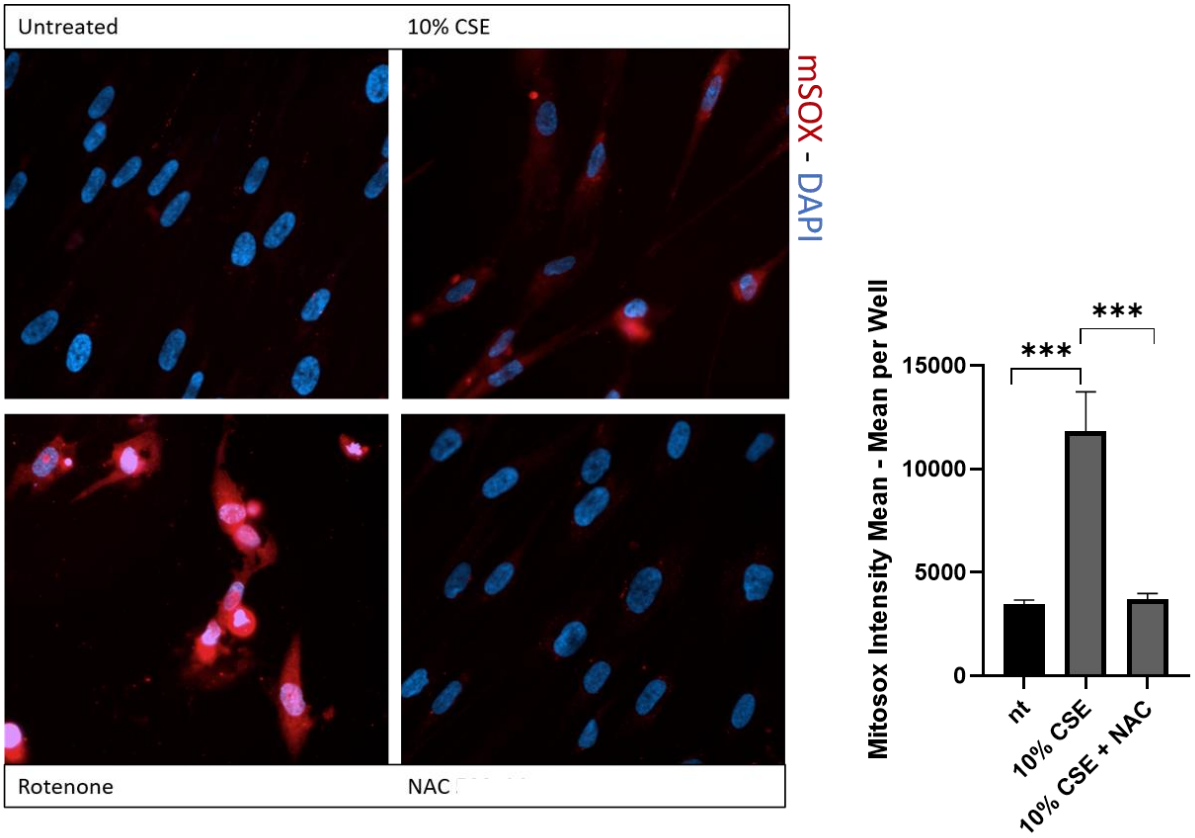

Fig.6: Production of mitochondrial superoxide. *MitoSox Red assay, Live cells imaging technique performed 72h after CSE stimulation. MRC-5 were treated with 10% CSE in the presence or not of NAC 500µM; Rotenone 10µM was added 24h as positive control. Confocal microscope Operetta CLS-Perkin Elmer was used to analyse the images, analysis is reported in the graph as mitoSox intensity mean per well. Magnification 40x. nt, no-treated.*

1.2. Investigation of Inflammasome components and Gasdermins expression and activation

The expression of inflammasome components was investigated. RT-qPCR was run for evaluating the gene expression of NLRP3, GSDME, GSDMD and pro-IL-1β under basal conditions and upon stimulation with CSE. Protein levels were measured by western blot for NLRP3, pro-IL1β and GSDME. WB data showed that NLRP3 and pro-IL-1β were undetected (Fig. 7). RT-qPCR confirmed the absence of NLRP3. ELISA assay showed no release of IL-1β and IL-18 (data not shown) after CSE stimulation.

Investigating gasdermins in lung fibroblasts stimulated with cigarette smoke is important due to the role of cigarette smoke in activating gasdermins, which are involved in inflammatory cell death. Research has shown that cigarette smoke can induce the activation of gasdermin D in

bronchoalveolar macrophages and bronchial epithelial cells, leading to pulmonary inflammation and remodeling[156,157] and caspase-3 is known to activate GSDME[158] therefore the expression of full length gasdermins E and D was investigated using RT-qPCR (Fig.7). Under basal conditions, GSDME gene expression was ten folds higher than GSDMD (Fig.7A). Both GSDMD and GSDME did not show significant modulations in response to CSE (data not shown). Constitutive expression of GSDME was confirmed by western blot. Cleaved GSDME ($GSDME^{NT}$) was observed after stimulation with 10% CSE for 72h. Treatment with zIETDfmk resulted in the inhibition of GSDME cleavage (Fig.7B).

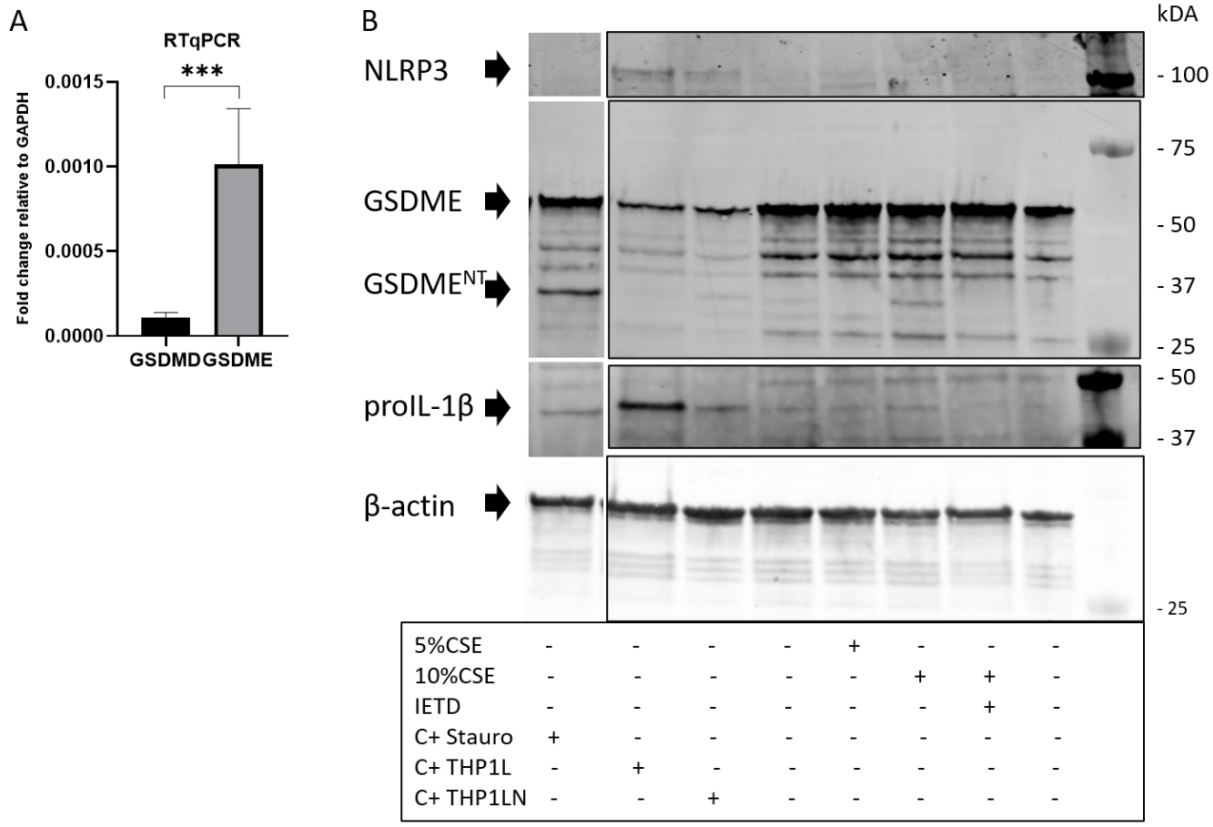

Fig. 7: Inflammasome components and GSDME expression. ***A****. RTqPCR of GSDME and GSDMD under basal conditions.* ***B****. MRC-5 cells were stimulated with CSE for 72h, 0.1 µM z-IETD-fmk was added 1h prior of stimulation with CSE. Western blot analysis was performed for pro-IL1ß, NLRP3 and GSDME. THP1 macrophages treated with LPS or LPS/Nigericin and MRC5 treated with Staurosporine were used as positive control.*

1.3. Impact of CSE on extracellular matrix remodeling

In COPD the functions of lung fibroblasts are altered in multiple ways, to investigate the myofibroblasts activation and their involvement in ECM remodeling we explored the impact of CSE on the expression of αSMA, COL I, and fibronectin in MRC-5 cells stimulated with 10% CSE for 72h. Elisa assays were used to detect and quantify the release of fibronectin (FN) and collagen I (COL-I). CSE 10% decreased COL-I and FN release, treatment with z-IETD showed to significantly restore the release of both proteins, NAC restored the release of COL-I (Fig.8A). Immunofluorescence staining was used for αSMA (data not shown), FN and COL-I expression, the images observed showed decrease in protein expression Fig.(8B).

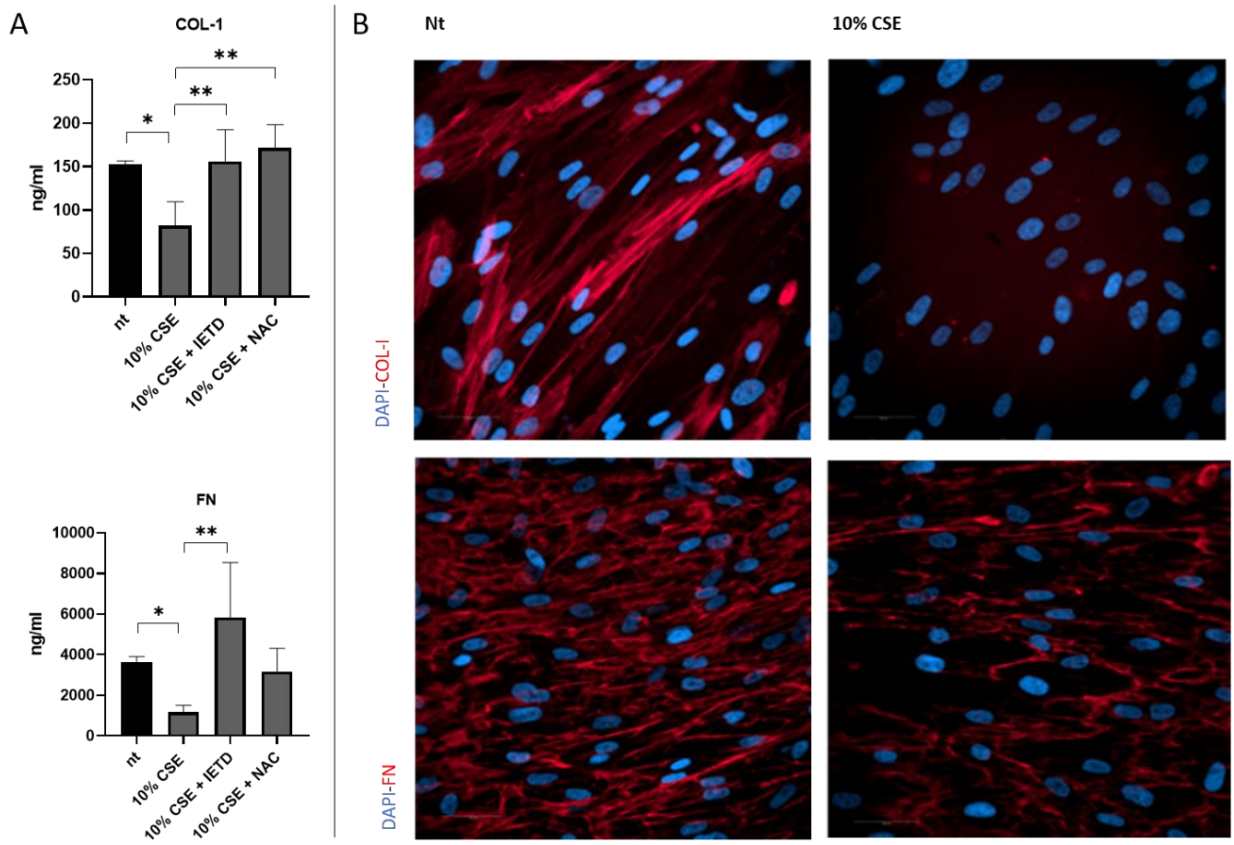

Fig.8: Impact of caspase activation on remodelig. ***A.*** *ELISA of FN and COL-I of MRC-5 stimulated with CSE for 72h. Z-IETD-fmk was used 1h prior of CSE, NAC was added simultaneously with CSE.* ***B.*** *Immunofluorescence staining of COL-I and Fibronectin was performed after stimulation with CSE 72h. - Operetta CLS-Perkin Elmer microscope was used to take the pictures. Magnification 40x. nt, no-treated.*

2. Validation of key findings in patient-derived primary human lung fibroblasts (phLFs)

2.1. Cigarette smoke induced caspase activation

Primary lung fibroblasts from peripheral lung tissue from subjects undergoing lung transplantation or tumor resection surgery were used. Resected lung tissue was isolated from an area distal from the tumor and that was macroscopically and histologically normal. Patients Characteristics are represented in Table T1.

Table T.1 Characteristics of patients UMCG

	Age	Gender (M/F)	Pack/years	FEV1 % pred	FEV1/FVC %
no smokers	64.9±12.7	2/8	-	101.9±15.1	77.9±6.4

Activation of caspase-1, -8, and -3/7 in response to cigarette smoke extracts (CSE) in N=10 phLFs was evaluated. Cells were treated with CSE at 5% and 10% for 72h. CSE induced a dose-dependent increase of caspase-1 and -8 activity (Fig.9B). LDH assays showed that 5% CSE did not induce cell death. phLFs exposed to 10% CSE displayed some mortality although the increase in LDH release did not reach statistical significance (Fig.9A).

There was no induction of caspase-3/7 activity and no cleavage of GSDME was observed (data not shown).

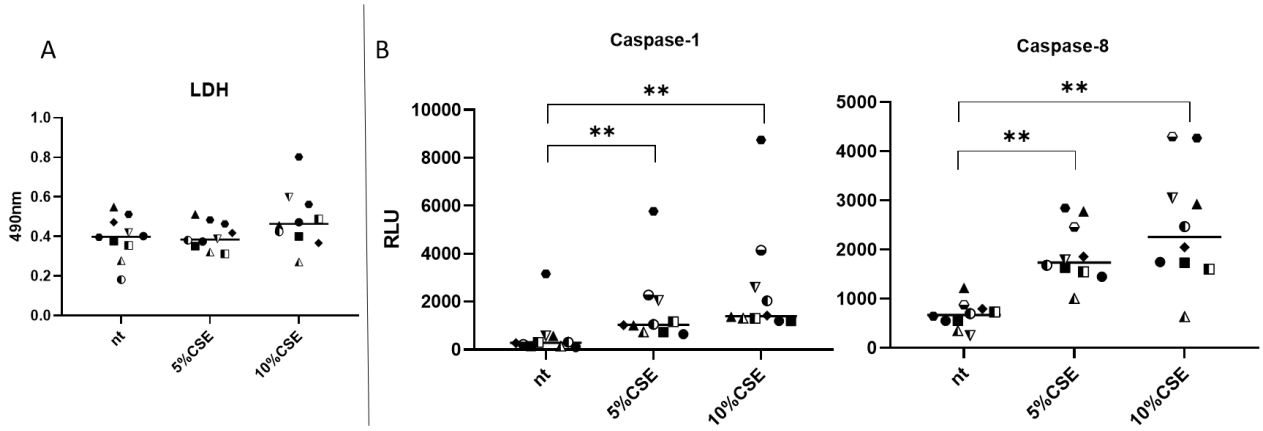

Fig.9: Impact of CSE on caspase activity and cell death. *N=10 phLFs were stimulated with 5% and 10% CSE for 72h.* ***A.*** *LDH assay was run in the supernatants after 72h stimulation* ***B.*** *The extracellular activity of caspase-1 and caspase-8 was investigated using an enzymatic assay.*

2.2. Explore connection between caspase-8-3/7 and ECM remodeling

Based on previous report connecting GSDM activation and fibrosis[91,93,159–162], as well as on the expertise of Prof. Brandsma group, we decided to explore the impact of the caspase-8 inhibitor IETD on CSE-dependent expression of alpha-SMA and release of fibronectin, decorin, TSP1 and ADAMTS1 in phLFs. Recent studies revealed that in COPD the functions of lung fibroblasts are altered in multiple ways. Airway remodeling is characterized by epithelial cell damage, mucus hypersecretion, increased airway smooth muscle mass (cell size and number) and altered deposition of ECM proteins (collagens, decorin, and elastin)[163]. Myofibroblasts (αSMA+) persist in the remodeled site, increasing the deposition of collagen type I and fibronectin. CSE increased markers of fibrosis in human primary lung fibroblasts obtained from donors[164]. TSP1 has roles in regulating cell adhesion, cell migration, apoptosis, ECM organization, activity of matrix-degrading enzymes., ADAMTS1 protease remodels the ECM through the proteolytic degradation of key substrates such as chondroitin-sulfated proteoglycans and collagen[165,166]. Expression of aSMA and Fibronectin was evaluated by IHC. Data showed changes in in protein deposition in the untreated versus CSE treated (Fig.10). However, changes were not quantifiable[167]. From a qualitative analysis, IETD appeared not to have impact on CSE-induced alterations.

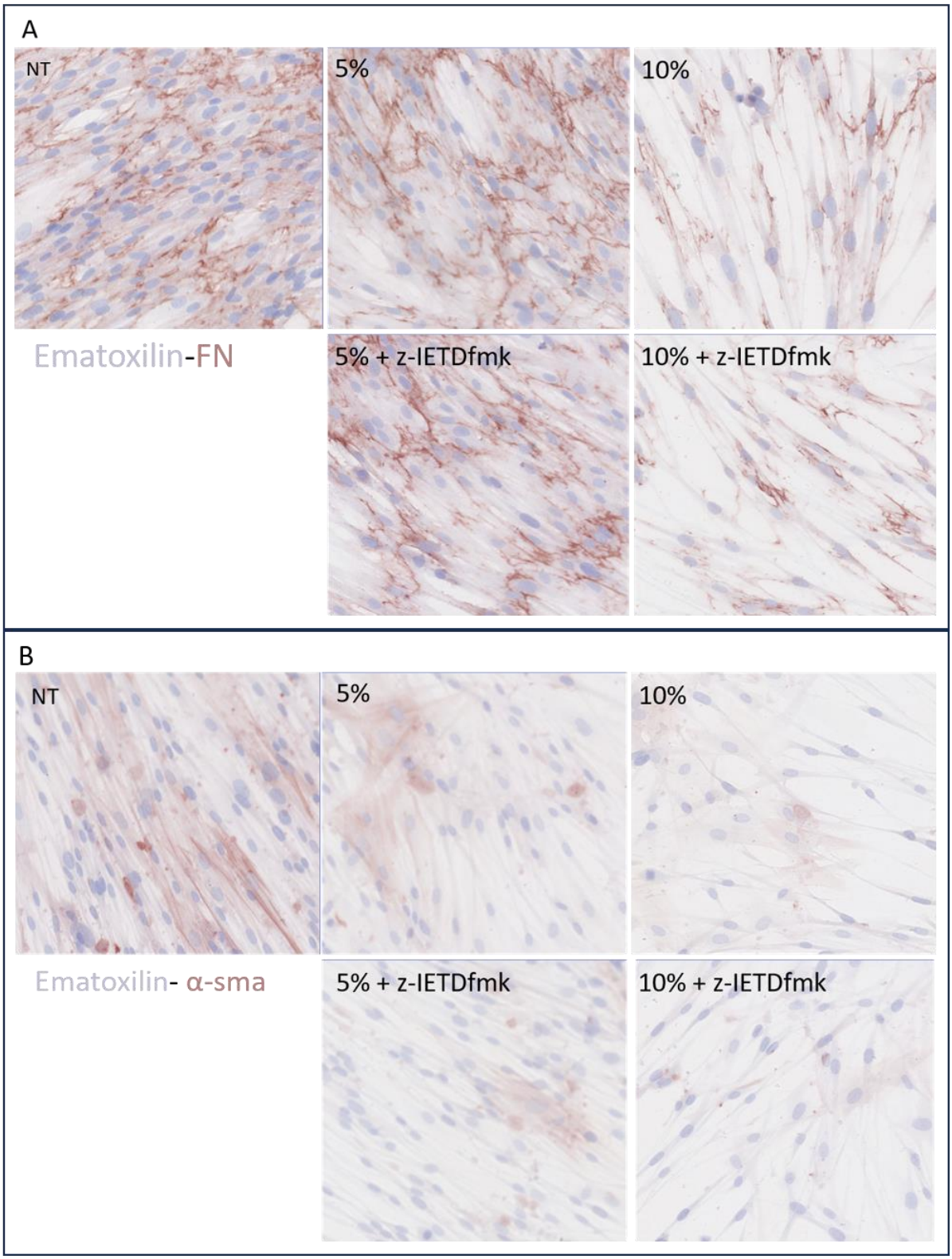

Fig.10: Fibronectin and alpha-SMA. *N=8 phLFs were seeded on coverslips and were exposed to 5% and 10% CSE, 1h before CSE stimulation cells were treated with 0.1µM of Z-IETD-FMK. Coverslips were fixed and stained using **A**. fibronectin antibody (MAB1940; 1:100). **B**. α-SMA antibody (clone asm-1, DAKO; 1:50). Pictures were taken using Nanozoomer whole slide scanner Hamamatsu. Magnification 20x.*

ELISA assays were used to detect and quantify the release of ADAMTS1, decorin, and TPS1. CSE 5% and 10% increased the release of ADAMTS-1 and TSP1 in N=10 (Fig.11 A,B), IETD treatment did not show significant inhibition for both proteins (data not shown). Increasing N will be required to have more solid data. phLFs did not show any changes in the Decorin release in response to CSE or to IETD (data not shown).

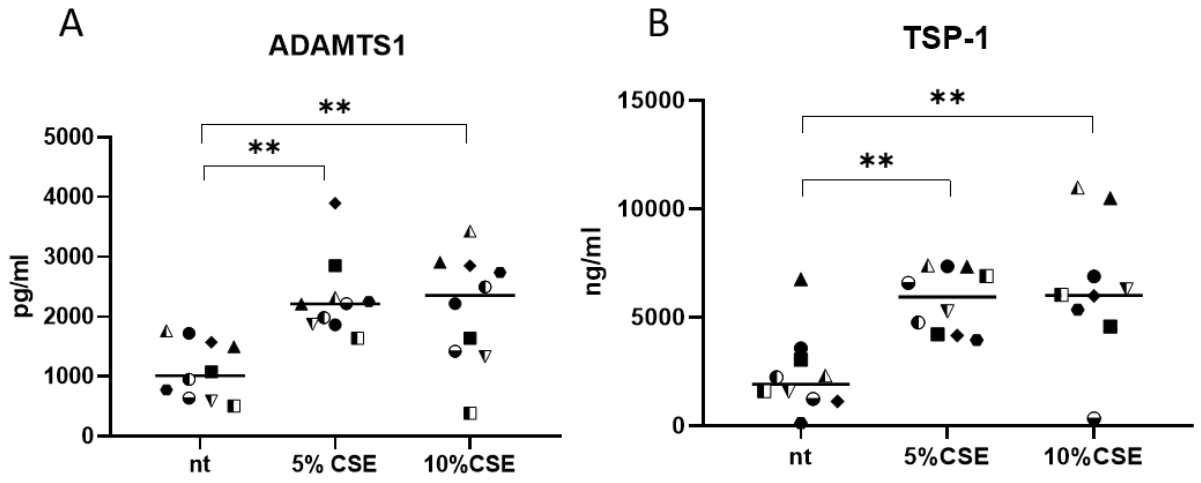

Fig.11: CSE increased the release of ADAMTS1 and TSP1. *N=10 phLFs were stimulated with 5% and 10% CSE for 72h. Surnatants were harvested and analyzed using ELISA assays **A**. ADAMTS1 **B**. Thrombospondin-1.*

ELISA assays were used to detect and quantify the release of FN and COL-I in N=10 phLFs. Results showed that CSE 10% decreased the release of FN and COL-I, IETD did not show to revert the decrease (Fig.12).

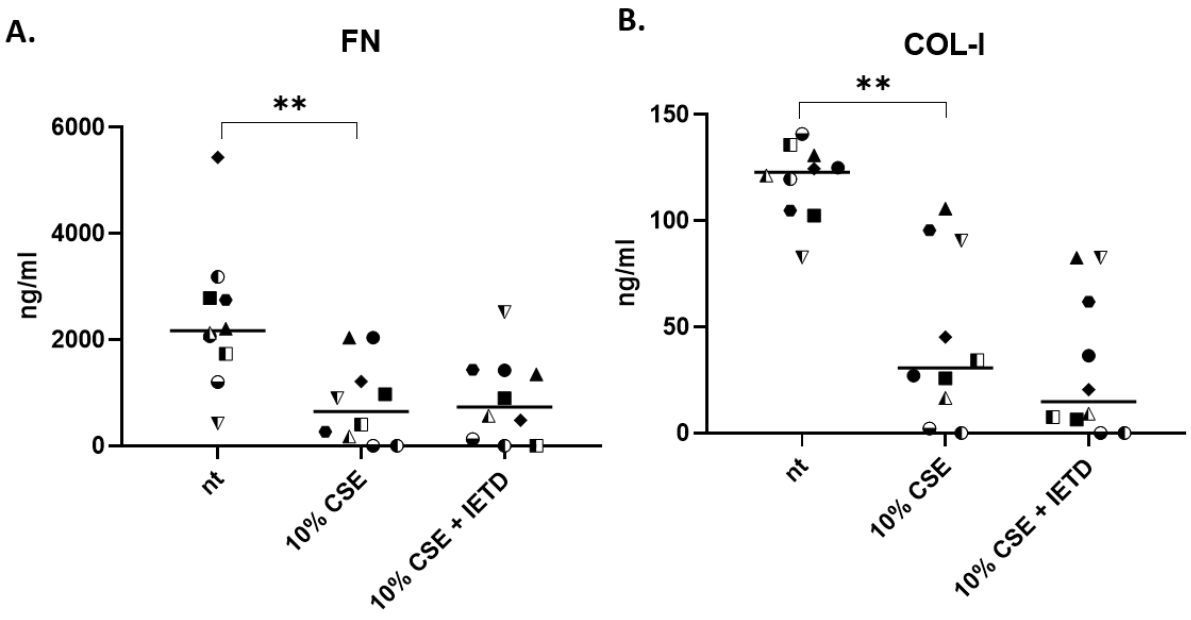

Fig.12: CSE decreased the release of FN and COL-1. *N=10 phLFs were stimulated with 10% CSE for 72h. z-IETD-fmk was used 1h prior of CSE. Surnatants were harvested and analyzed using ELISA assays **A**. FN **B**.COL-I.*

Preliminary data in N=3 phLFs showed that CSE 10% decreased the release of FN and COL-I and treatment with NAC restored the basal condition of both proteins released, IETD did not show any change (Fig. 13).

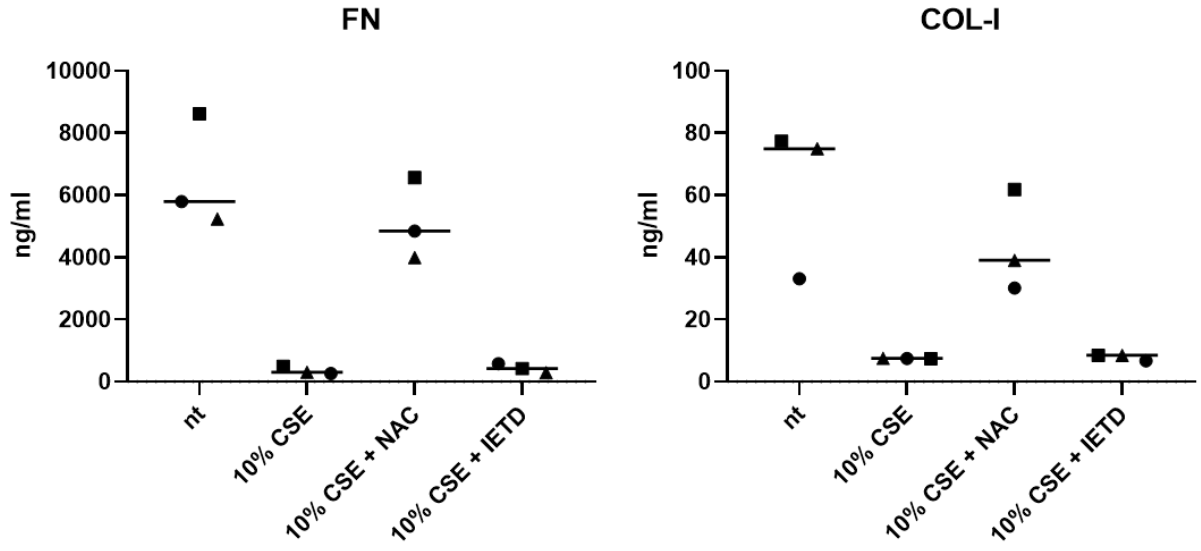

Fig.13: CSE decreased the release of FN and COL-1, preliminary data. N=3 phLFs were stimulated with 10% CSE for 72h. z-IETD-fmk was used 1h prior of CSE NAC was used simultaneously with CSE. Surnatants were harvested and analyzed using ELISA assays **A**. FN **B**.COL-I.

2.3. Explore the connection between the caspase-8-3/7 and senescence

Evidence suggests that in aging cells there is a naturally occurring increase in inflammasome protein expression [168]. Very little is known regarding the connection between caspase activation and senescence. [96]. During senescence cells stop dividing to prevent tissue damage and tumorigenesis, upon aging the number of senescent cells increases in tissues. Cells in a senescent state can secrete inflammatory factors that disturb tissue repair and homeostasis. CSE has been showed to increase cellular senescence in different cell types[169–171]. The percentage of senescence-associated β-galactosidase-positive cells is increased in multiple cell types in COPD patients, including airway epithelial cells, smooth muscle cells, endothelial cells, and fibroblasts, as well as in CSE-treated alveolar and bronchial epithelial cells. Another senescence marker, the cell cycle inhibitor p21 was found to be increased in total lung tissue, alveolar cells, smooth muscle cells, endothelial cells, and leukocytes of COPD patients; p21 was also increased in CSE-treated bronchial epithelial cells and fibroblasts[171 172].

Therefore, considering previously published work as well as the expertise of Prof. Brandsma's group, we explored β-GAL and p21 as markers of CSE-induced senescence and the effect of the caspase-8 inhibitor IETD. As a positive control for senescence, we used paraquat-stimulated pHLFs. Paraquat exposure is a risk factor for COPD, and it can induce senescence specifically via mitochondrial reactive oxygen species production [173 174,175].

The percentage of senescence-associated β-galactosidase-positive cells was significantly increased after CSE and paraquat treatments [176] (Fig.14 A, B) IETD did not revert CSE-induced β-gal increase (Fig.15A). Exploration of p21 did not produce consistent results, further analysis will be necessary.

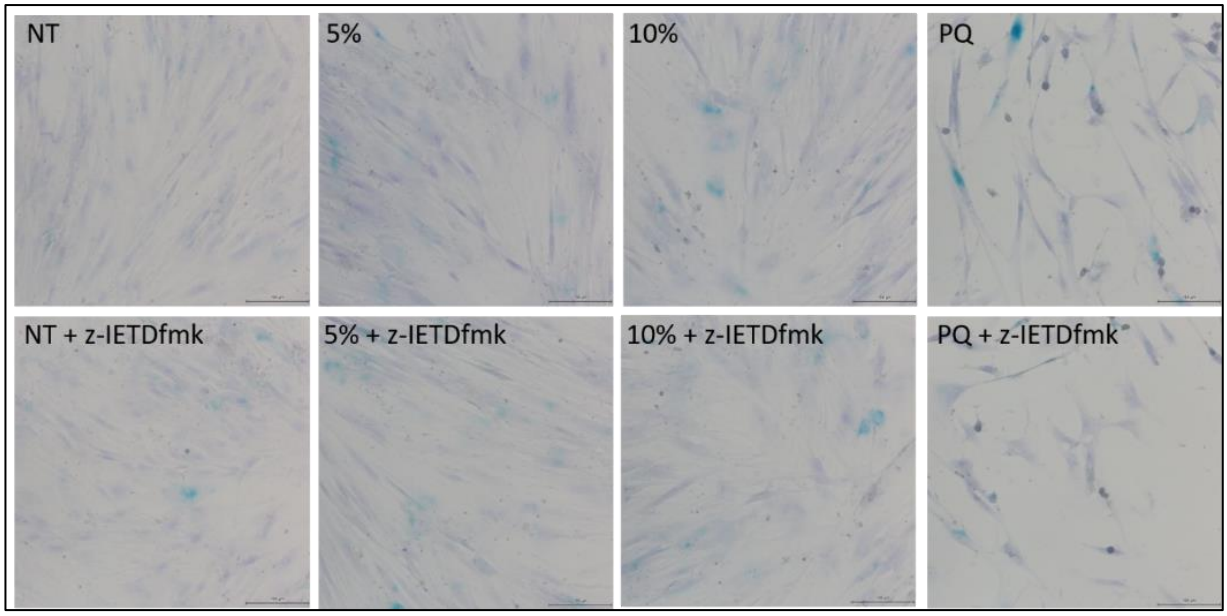

Fig.14: **SA-β-gal staining.** *N=10 phLFs were exposed to 5%, 10% CSE, and N=9 were exposed to paraquat (PQ, 100µM 24h), 1h before CSE or PQ stimulation cells were treated with 0.1µM of Z-IETD-FMK. After 72h cells, Cellular senescence was assessed with standard SA-β-gal staining. Four random images of every well with cells were taken using Zeiss AxioObserver Z1, Tissue Fax scanner objective Zeiss- LD "Plan-Neofluar" 20x/0,4 Corr Dry, Ph2 at a total magnification of ×200.*

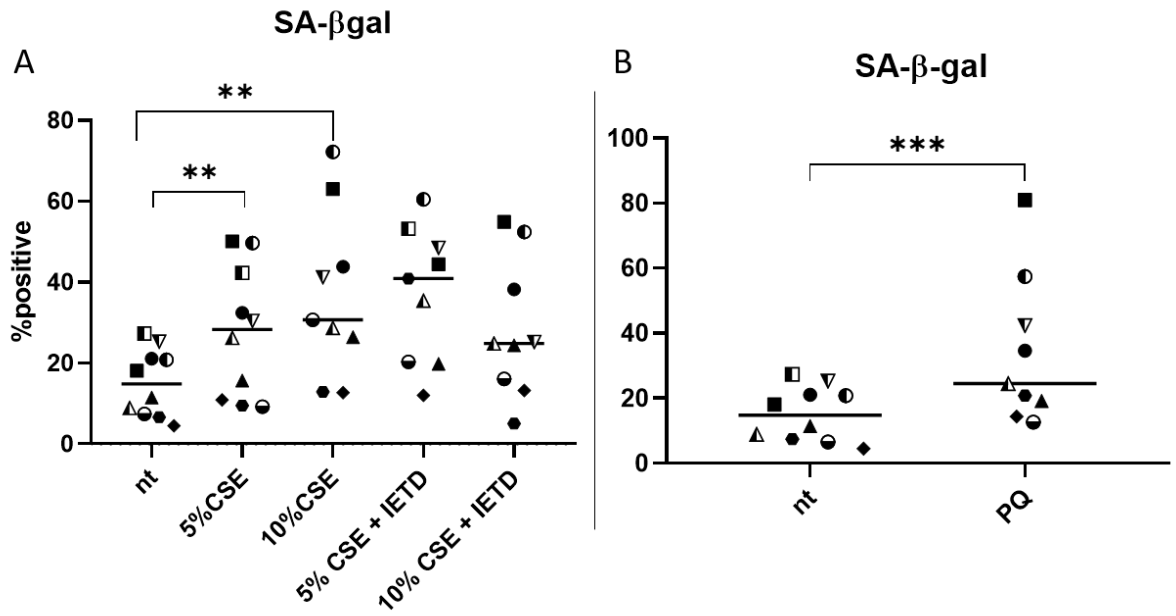

Fig.15: Percentage of senescence-associated β-galactosidase-positive cell. *SA-β-gal-positive cells and total cells were scored blindly to calculate the percentage of SA-β-gal-positive cells.* ***A****. N=10 phLFs were treated with CSE for 72h, zIETD-fmk was added 1h prior of CSE.* ***B****. Comparison between No-treated and PQ treated, PQ was added for 24h.*

2.4. Start a collection of patients derived human lung fibroblasts (phLFs)

As part of the PhD project, I was trained by Prof. Fabio Bucchieri and Alberto Fucarino, PhD to how to isolate and grow fibroblasts from fresh lung resections. The study was conducted in collaboration with ISMETT IRCCS (the study protocol was approved by the Institutional Review Board for human studies at IRCCS ISMETT, # IRRB/19/19). Fresh lung tissue samples were obtained from patients undergoing surgery for lung cancer (areas well distant from the tumor were used for this study). N=23 phLFs were isolated from patients with normal lung functions. N=10 from smoker patients, N=4 from ex-smokers and N=9 from no-smoker subjects, patient characteristics are shown in the Table T2.

Table T2. Characteristics of patients, RiMed/ISMETT

	Age	Pack/years	FEV1 L	FEV1 % pred	FEV1/FVC %
Smokers (N=10)	68.4±7	48.7±13	2.6±0.64	103.8±8	76.1± 5.2
Ex-Smokers (N=4)	75	45±21.2	2.1±0.97	86.5±7.77	75.7±0.35
No-Smokers (N=9)	62.8 ±9	-	2.2±0.56	98.9±15.6	80.3±12
Smokers COPD	79.5±6.3	19.3±1.15	31.7±42.8	52±1.41	30.5±16
Ex-smokers COPD	67±6.1	45±7	1.7±0.5	63±20	39.2±7.8

After isolation, phLFs were expanded until confluency and characterized by flow cytometry. To this purpose cells were stained in darkness with fluorescent-tagged antibody specific for CD90 which is a small membrane glycophosphatidylinositol (GPI) anchored protein, highly expressed in fibroblasts and with fluorescent-tagged antibody specific for EpCAM or CD326 a cell adhesion molecule which is a marker specifically expressed in epithelial cells. The samples were analyzed by flow-cytometry using CytoFLEX (BeckmanCoulter, Brea, CA, USA). Cell phenotype characterization confirmed the isolation of phLFs positive for CD90, and negative for EPCAM (Fig.16).

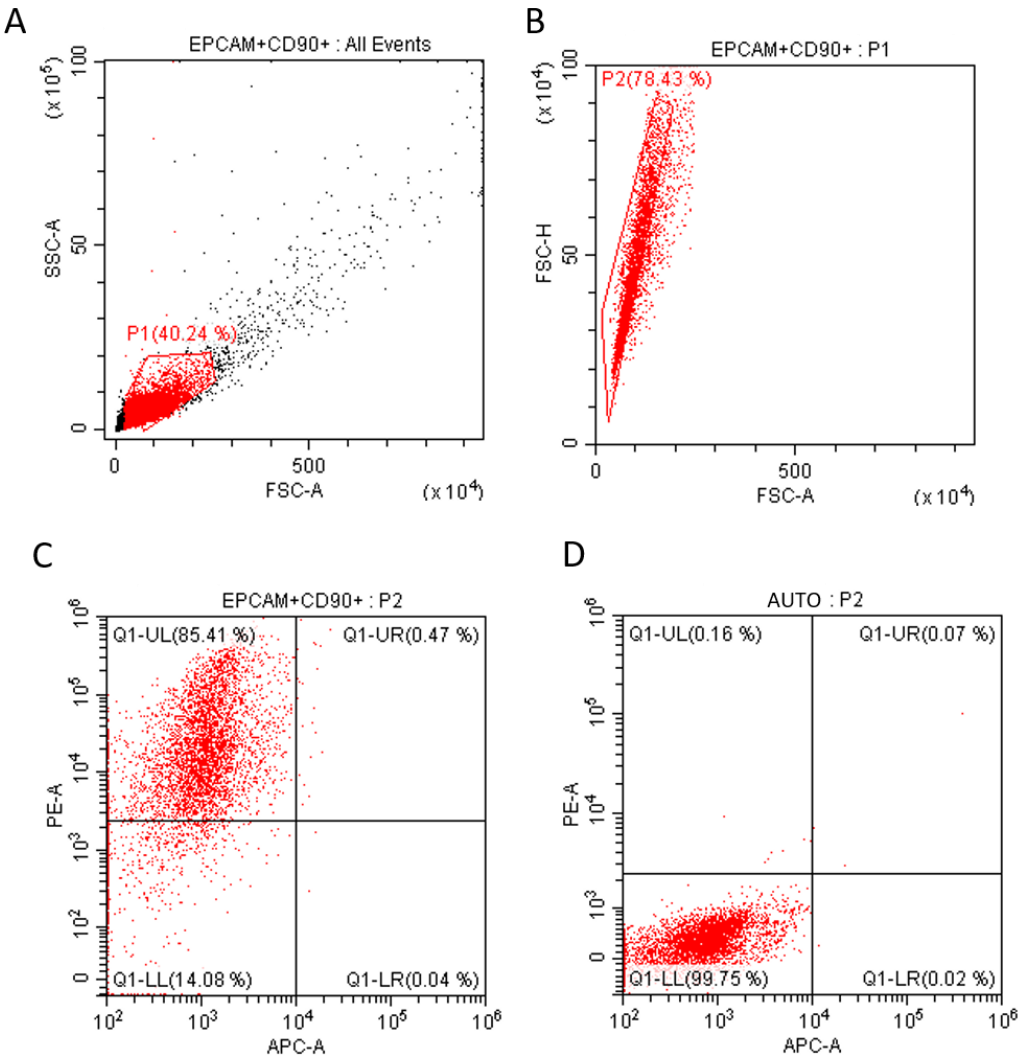

Fig.16: Characterization of phLFs by flow cytometry. *Cells were stained in darkness with 1µl of fluorescent-tagged antibody specific for CD90 and with 1µl of fluorescent-tagged antibody specific for EpCAM or CD326. The samples were analyzed by flow-cytometry using CytoFLEX.* ***A-B****. Gating strategy to select cell population.* ***C****. Extracellular markers, CD90 (PE) and EPCAM (APC) were used to evaluate the percentage of positive cells.* ***D****. Dot plot showing autofluorescence of unstained cells. FSC, forward scattering. SSC, side scattering.*

3. Evaluate cleaved GSDMD and caspase-3 in lung tissue sections

The third objective of my PhD involved investigating downstream events following caspase activation in response to cigarette smoke extract (CSE) in peripheral lung tissues from both smokers and non-smokers, utilizing immunohistochemistry. This approach aimed at bridging the gap between cellular studies and the actual tissue context. However, the assessment of lung fibroblasts using this method faced challenges in lung parenchyma tissue sections. The inadequate dispersion of lung fibroblasts presented difficulties in accurately marking them with IHC. Given the crucial role of macrophages in the inflammatory response, and considering their higher abundance in the tissue area, the decision was made to move the focus to macrophages.

3.1. Gasdermin D and caspase-3 in lung sections from smokers, no-smokers and ex-smoker patients

Data collected by Buscetta et al. indicated that exposure of hMDMs to CSE promotes the activation of multiple caspases leading to GSDMD cleavage.

We therefore hypothesized that cleaved GSDMD may be increased in lung macrophages of smoking subjects. Using an antibody specific for cleaved GSDMD, we performed IHC analysis on distal lung tissue sections derived from three small study groups: smokers (n= 6), ex-smokers (n= 5), and no-smokers (N=3), characteristics of the patients are shown in Table T3.

Table T3. Characteristics of patients

	Age	Gender (M/F)	Pack/years	FEV1 L	FEV1 % pred	FEV1/FVC %
Smokers (N=6)	64.7 ± 4	3/3	27.2 ±12	2.4 ±1	98.8 ±16	92.2 ±9
Ex-Smokers (N=5)	65.6 ±5	4/1	46.6 ±30	2.3 ±0.3	85.5 ±5	91.3 ±6
No-Smokers (N=3)	63.3 ±4	1/2	0	2.6 ±1	114.7 ±13	116 ±2

As shown in Fig.17, the percentage of lung macrophages positively stained for GSDMD-NT was significantly higher in smokers compared to ex-smokers and no-smoking controls.

These data were used as a contribution to the article “Cigarette smoke promotes ASC-independent activation of multiple caspases leading to gasdermin cleavage and mitochondrial damage in human macrophages” published in 2022, FASEB Journal, M. Buscetta, M. Cristaldi,

M. Cimino, **Agnese La Mensa**, P. Dino, F. Bucchieri, F. Rappa, S. Amato, T. S. Aronica, E. Pace, A. Bertani, C. Cipollina[81].

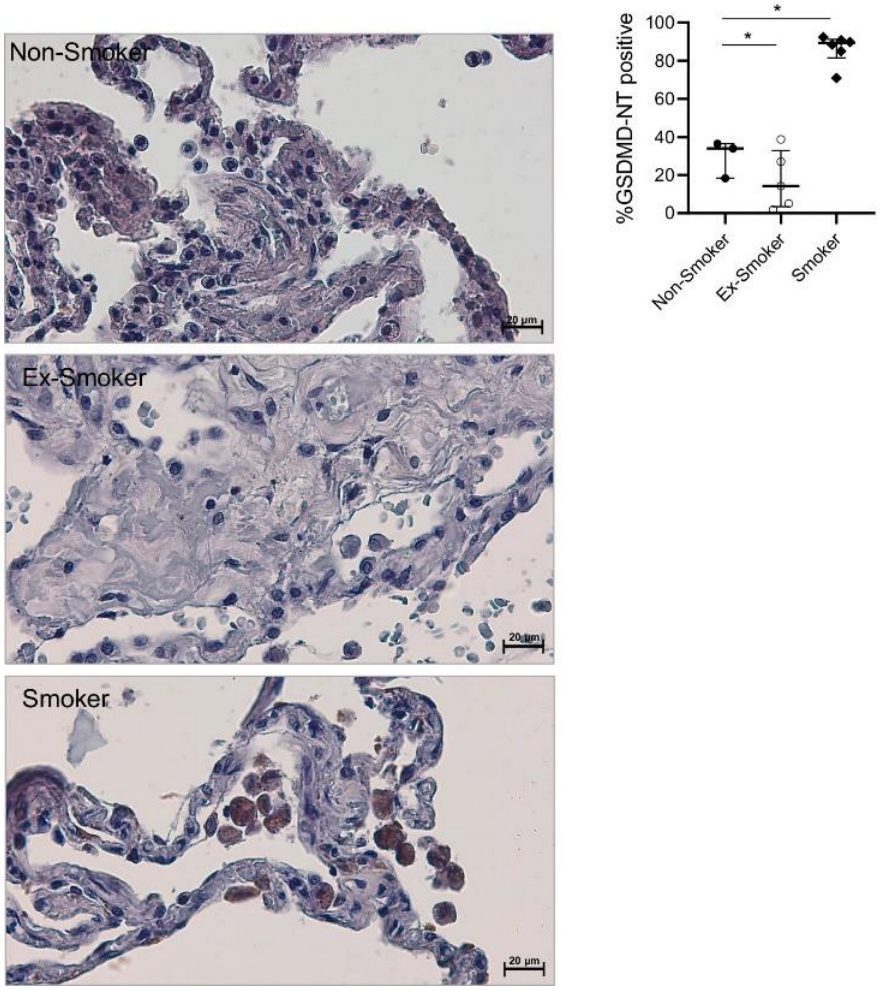

Fig.17: Cleaved GSDMD is increased in lung macrophages from smokers. *Representative images of immunohistochemical staining of distal lung tissue sections using an antibody specific for GSDMD-NT. The graph shows the percentage of cells positive for GSDMD-NT. Data are presented as median with interquartile range. One-way ANOVA followed by the Bonferroni post hoc test for multiple comparisons was selected as an appropriate method for data analysis.*

We next evaluated whether cigarette smoking may promote the activation of caspase-8/caspase-3 pathway in human lung macrophages. To this purpose, activation of caspase-3 was evaluated by immunohistochemistry, using an antibody specifically recognizing cleaved caspase-3, in lung tissue sections of smoking subjects (N = 5). Results were compared with those obtained in non-smoking controls (N = 6). Characteristics of patients are in Table T4.

Table T4. Characteristics of patients

	Age	Gender (M/F)	Pack/years	FEV1 L	FEV1 % pred	FEV1/FVC %
No-Smokers (6)	62 ± 8.8	1/5	-	2.4 ± 0.7	116 ± 15.6	106.6 ± 13.2
Smokers (5)	63 ± 4.5	2/3	31 ± 15.6	2.4 ± 0.5	107.2± 9.7	89.1 ± 10.9

As shown in Fig.18, the percentage of macrophages positively stained for cleaved caspase-3 was significantly higher in Smokers compared to No-Smoker controls. These data were used as a contribution to the article: "Caspase-8 activation by cigarette smoke induces pro-inflammatory cell death of human macrophages exposed to lipopolysaccharide." Published in 2023, Cell Death Dis., M. Cristaldi, M. Buscetta, M. Cimino, **Agnese La Mensa**, M. R. Giuffrè, L. Fiore, C. Carcione, F. Bucchieri, F. Rappa, C. Coronnello, N. Sciaraffa, S. Amato, T. S. Aronica, G. Lo Iacono, A. Bertani, E. Pace, C. Cipollina[158].

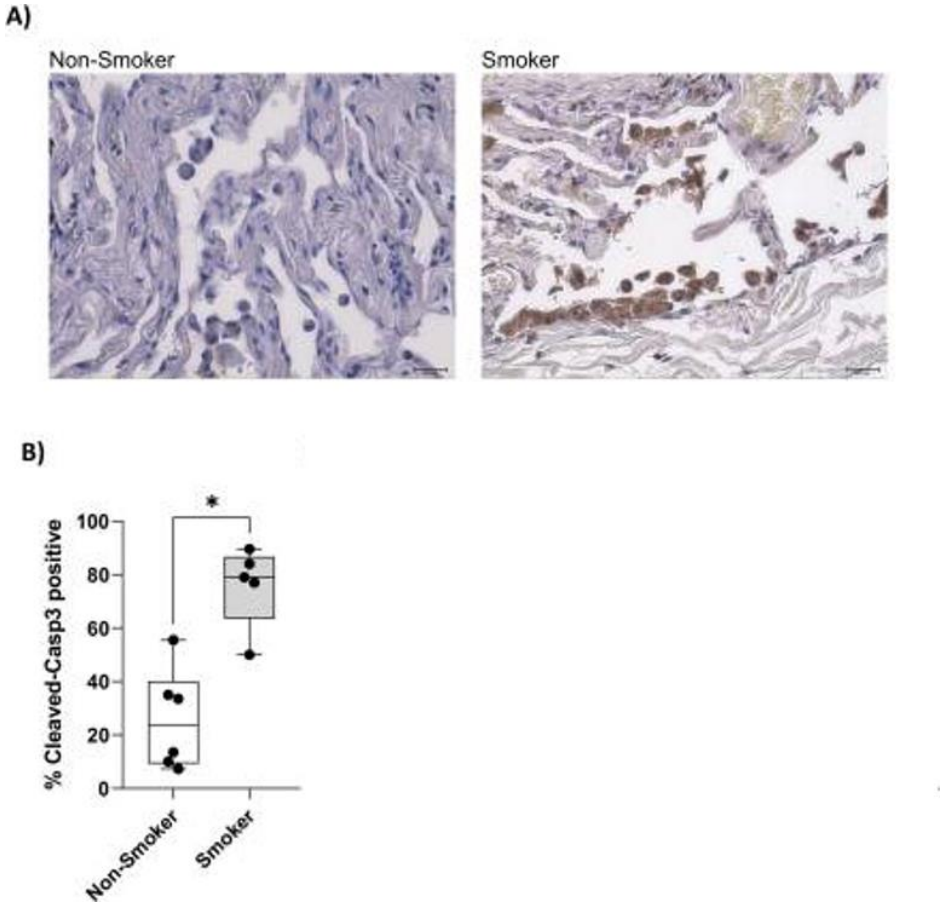

Fig.18: Cleaved caspase-3 and *GSDME* gene expression in alveolar macrophages from smokers compared to no-smoking controls. ***A.*** *Representative images of immunohistochemical staining of distal lung tissue sections of Smokers (N = 5) and No-smoking*

controls (N = 6), using a specific antibody for cleaved caspase-3. ***B.*** *Graph showing the percentage of cells positive for cleaved caspase-3. Data are presented as median with interquartile range. The difference between the percentage of immunopositivity in No-Smoking controls and Smokers was statistically evaluated with the Mann–Whitney test.*

3.2. GSDMD in disease associated with chronic inflammation (DACI) – contribution to Cost Action Mye-InfoBank CA20117

As part of my PhD project, I participated to the Cost Action Mye InfoBank CA20117. Myeloid immune cells are important mediators in the pathology of many diseases, especially in diseases associated with chronic inflammation (DACI). Recent advancements in molecular profiling technologies have led to the generation of large data sets, many of those not fully explored yet, but accessible to the entire scientific community via public data repositories. It is the aim of this COST Action to repurpose those data sets, retrieve and curate myeloid cell-specific information, and apply this information to develop novel biomarkers for DACI. To this end, Mye-InfoBank utilizes COST networking tools to enable the interaction of molecular biologists, bioinformaticians, immunobiologists, biobank coordinators and clinicians. The concerted activity of these experts on myeloid cell biology (either basic or clinical research) MYE, bioinformatics INFO, and bio-banking BANK, will transform complex molecular information into standardized and applicable biomarkers, which have the potential to improve clinical decision-making in several socio-economically important diseases.

My contribution so far was related in particular to two short-term missions (STSM), one based at IGTP in Badalona, Spain, and the second at Oslo University Hospital, Oslo, Norway.

Short-term Scientific Missions (STSMs) are exchange visits for researchers within their Action. This exchange program facilitates individuals to conduct scientific activities at an institution or laboratory based in a different country, which is also part of the Action. One main output of the cost action is to facilitate the transformation of complex molecular data on myeloid cell signatures into biomarker panels employable in clinical diagnostic applications. To this end, immunostainings of tissue antigens offer the possibility to employ such panels in large collections of biosamples across research labs and are readily compatible with routine pathological examinations.

The first aim was to set the optimal IHC conditions for antigens analysis of FFPE specimens from inflammatory disease and cancer and to establish the standard operating procedures (SOPs) for their evaluation. The purpose of the second STSM was to combine the optimized FFPE-based immune staining protocols established in the preceding cell-type focused STSMs (macrophages in Badalona, DCs and TLS in Limerick, and neutrophils in Brussels) into four 6-plex panels that apply to larger sample collections by using an automated tissue staining platform. Here I will show preliminary results obtained from the first STSM.

We proposed cleaved GSDMD as marker for DACI. Recent findings suggest that GSDMD may be a potential target for therapeutic intervention in lung cancer. Research has shown that GSDMD plays a myeloid-cell-specific role in lung cancer metastasis, with GSDMD knockout mice exhibiting significantly fewer cancer foci in the lungs, decreased metastasis, and increased median survival rate[177]. Also, GSDMD expression was found to be upregulated in human non-small cell lung cancer (NSCLC) tissue, and its depletion reduced lung cancer growth[178]. Furthermore, GSDMD is involved in the release of IL-1β, which has been highlighted as having a crucial role in lung cancer[179].

We performed Immunohistochemistry (IHC) on paraffin-embedded tissue sections from Crohns (Inflammed/Non-inflammed), Lung, and colon cancer (Tumor/Non tumor) from 3 different patients, using anti-CD68, CD5L, CD169, cleaved Gasdermin D & Cathepsin L antibodies. The figure shows preliminary results obtained with cleaved GSDMD, in both colorectal and lung cancer macrophages staining was stronger than in non-tumor-adjacent tissue (Fig.19-20), non-inflamed region of the colon in Chron's disease displayed unspecific staining of endocrine cells in the crypt and paneth cells (Fig.18).

.

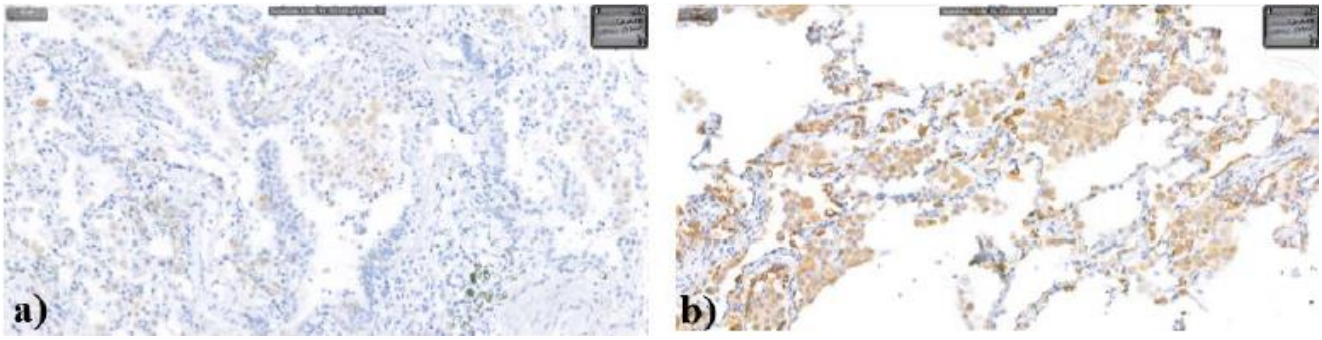

Fig.19: Cleaved GSDMD staining in Lung cancer. Preliminary results. *Representative images of immunohistochemical staining using a specific antibody for cleaved GSDMD* ***a)*** *Non-tumor adjacent lung cancer tissue.* ***b)*** *Lung cancer tissue.*

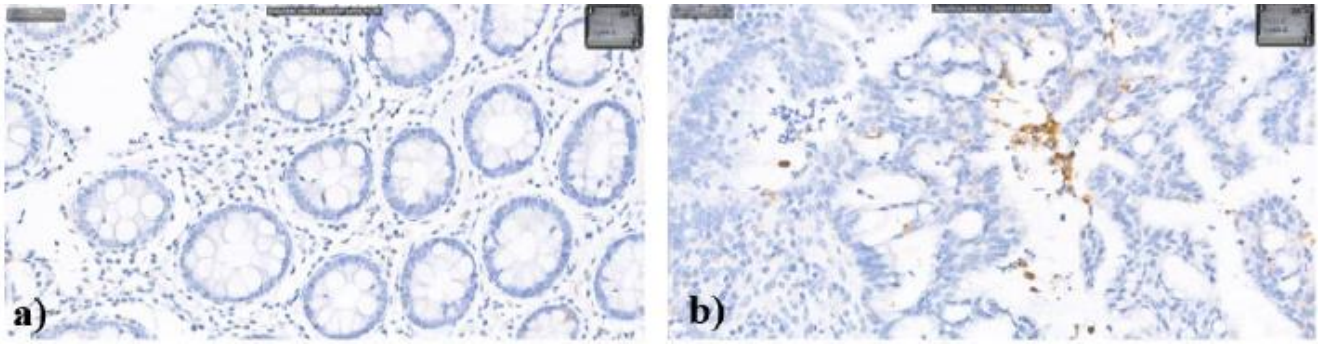

Fig.20: Cleaved GSDMD staining in colorectal cancer. **Preliminary data.** *Representative images of immunohistochemical staining using a specific antibody for cleaved GSDMD.* ***a)*** *Healthy tissue adjacent to colorectal cancer.* ***b)*** *Colorectal cancer tissue.*

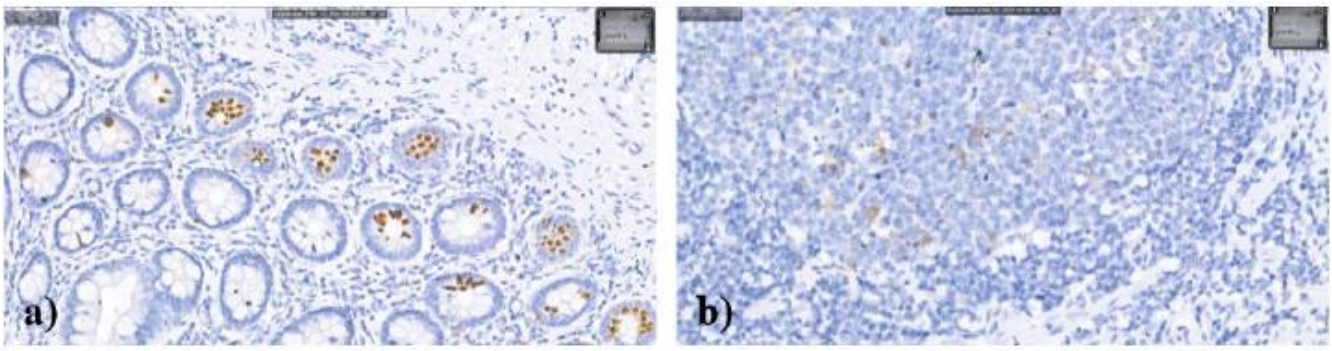

Fig.21: Cleaved GSDMD staining in Chron's disease. Preliminary data. *Representative images of immunohistochemical staining using a specific antibody for cleaved GSDMD* ***a)*** *Non-inflamed region of the colon in Chron's disease* ***b)*** *Chron's disease tissue.*

Discussion

Exposure to cigarette smoke constitutes a major risk factor for the development of most lung diseases, such as chronic obstructive pulmonary disease and lung cancer. The damaging effects of CS are manifested in the disruption of the epithelial barrier, histological alterations including epithelial remodeling and sub-epithelial fibrosis of small airways, oxidative stress-induced damage to proteins and organelles, and an acceleration of the aging process within the lungs. The cumulative consequences of these processes contribute significantly to the pathogenesis of COPD [9,10]. The specific relationship between cigarette smoke and inflammasome-related response in human lung fibroblasts has not been directly addressed in literature so far. Growing evidence suggests that cigarette smoke activates the NLRP3 inflammasome in the lung epithelium, with increased expression of NLRP3, pro-IL-1β, higher caspase-1 activity, and increased release of inflammasome-related cytokines IL-1β and IL-18[33–35]. Macrophages appear to respond differently as cigarette smoke extract exposure inhibits inflammasome activation and reduces the release of IL-1β and IL-18 [36,37]. The study conducted by Buscetta et al. showed that CS promotes inflammasome-independent activation of caspase-1 and -4 leading to GSDMD cleavage and pyroptosis in human macrophages, further elucidating the complexity of CS-induced cellular responses [38,81,158].

This study endeavors to extend the existing body of knowledge by directly addressing the specific relationship between CS and inflammasome-related responses in human lung fibroblasts. Utilizing MRC-5, a human fetal lung fibroblast cell line, as the experimental model, the investigation aimed to investigate the NLRP3 inflammasome activation and downstream responses in human lung fibroblasts exposed to cigarette smoke extracts. Upon exposure to cigarette smoke extract, activation of caspase-1, -8 and -3/7 was observed in MRC-5 cells. This prompted an exploration of the upstream events, revealing that caspase-1 was activated independently of NLRP3 inflammasome and caspase-8, while caspase-3/7 activation was identified to be caspase-8 dependent. An antioxidant and cytoprotectant was added to the study, N-acetylcystein, which not only inhibited all caspase activities but also mitigated reactive oxygen species in the mitochondria. This critical observation linked caspase activation directly with oxidative stress and mitochondrial damage in the MRC-5 cell line.

We observed constitutive expression of the inflammasome adaptor ASC and caspase-1, while NLRP3 and pro-IL-1β remained undetected. This was further substantiated by RT-qPCR, which

confirmed the absence of NLRP3 (supported by the human lung cell atlas[180]), and ELISA assays, which demonstrated no release of IL-1β and IL-18 following CSE stimulation. These data conclusively excluded the presence and activation of the NLRP3 inflammasome pathway post-CS exposure in MRC-5 cells.

Venturing into uncharted territory, the investigation sought to unravel the expression and cleavage of gasdermin E in human lung fibroblasts, particularly in the context of CS exposure. GSDME, known to induce pyroptosis in macrophages, was discovered to be highly expressed in various structural cell types, including fibroblasts [181] and can be cleaved by Caspase-3 turning apoptosis into the pro-inflammatory pyroptosis[182]. The basal expression of GSDME was found to be ten times higher than that of GSDMD under normal conditions. Interestingly, while no significant modulations were observed in response to CSE, cleaved GSDME was identified post-stimulation. Notably, inhibition of Caspase-8 prevented GSDME cleavage, establishing the axis caspase-8 – caspase 3/7 – GSDME-NT as activated in response to CSE. This observation shed light on a novel facet of CS-induced cellular responses, unveiling a potential avenue for further exploration in understanding the intricacies of GSDME activation in lung fibroblasts.

The exploration of the pyroptotic role of GSDME [183] added yet another layer to the study's complexity. Live cell imaging using Sytox green, a nucleic acid stain, revealed an absence of pores in the cell membrane during CS exposure. This intriguing finding suggested a resistance to pyroptosis, as the probe was not internalized due to the lack of pores. This observation opened up avenues for further inquiry into the conditions under which GSDME may induce pyroptosis in lung fibroblasts.

Recognizing the pivotal role of fibroblasts in contributing to structural changes observed in COPD, particularly fibrosis and loss of lung elasticity, the link between caspases activation and differentiation in myofibroblasts[127,134,184] the study extended its investigation to the downstream effects of caspase-8-caspase-3/7 activation in correlation with airway extracellular matrix remodeling. CSE exposure induced a decrease in Collagen-I and fibronectin release, and treatments with z-IETD (caspase-8 inhibitor) and NAC effectively restored ECM homeostasis. These findings underscored the critical role of caspase-8-caspase-3/7 activation in ECM disruption in MRC-5 cells treated with cigarette smoke. The study's innovative approach in linking caspase activation to ECM remodeling provides novel perspectives on the mechanisms driving airway remodeling in the context of CS exposure,

contributing significantly to our understanding of the molecular events triggered by CSE in lung fibroblasts.

The correlation between the inhibition of caspase 8 and increased collagen production can be explained by the complex interplay between caspase activity, apoptosis, and collagen synthesis. While the traditional role of caspases is associated with apoptosis and cell death, emerging evidence suggests that caspases, including caspase 8, may have non-apoptotic functions. Studies in mice have shown that caspase 8 inhibition can lead to an upregulation of collagen and lamin in the extracellular matrix, resulting in increased stiffness and fibrosis[185]. Furthermore, S-nitrosylation of caspase-3 has been shown to be significantly higher in adhesion fibroblasts, and the decrease in caspase-3 activity due to S-nitrosylation is associated with the inhibition of apoptosis and increased collagen production[186]. In contrast, inhibition of apoptosis via caspase blockade has been linked to a significant reduction in CD45+Col-I+ cells, which are associated with collagen production[187].

This study showed, within the context of cigarette smoke exposure, that caspase-8-caspase-3/7 inhibition increased collagen I and fibronectin restoring the basal condition, linking the non-apoptotic role of caspases 8 and 3/7 with the maintenance of the ECM homeostasis. These findings highlight the need for further research to fully elucidate the complex and multifaceted roles of caspases in the context of cigarette smoke exposure and their impact on ECM homeostasis. Additionally, the study's results underscore the importance of considering non-traditional roles for caspases in the context of specific pathological conditions, such as cigarette smoke exposure, and the potential implications for developing targeted interventions to modulate caspase activity in the context of ECM remodeling. The findings align also with existing evidence on the impact of CSE on oxidative stress, apoptosis, and proteomic alterations in lung fibroblasts, further emphasizing the multifaceted and detrimental effects of CSE on cellular homeostasis and structural integrity.

To validate the observed phenomena in a more physiologically relevant setting, the investigation turned to primary human lung fibroblasts, isolated as described before[149] and treated with CSE. Results revealed that caspase-1 and caspase-8 activity was induced, instead caspase-3/7 was not, contrasting the caspase-3/7 activation observed in MRC-5 cells. The study explored senescence and identified CSE-induced β-galactosidase expression in phLFs. This finding offered a potential explanation for the observed lack of caspase-3/7 activation, may be due to cell senescence, leading to resistance to apoptosis in phLFs [188,189]. This

contextual understanding highlights the dynamic nature of CS-induced responses, with cellular context playing a crucial role in dictating the observed outcomes.

The investigation further dissected the complexities of ECM remodeling in phLFs, revealing decreased fibronectin and Collagen-I levels post-CSE treatment. Intriguingly, there was an increase in the expression of ADAMTS-1 and TSP1, and inhibition of Caspase-8 did not restore basal conditions. Preliminary results employing NAC, however, demonstrated promise in restoring fibronectin and Collagen-I to basal conditions.

These results align with existing research on the modulation of collagen and fibronectin production. Studies have shown that the antioxidant epigallocatechin-3-gallate (EGCG) and NAC have promising potential in modulating collagen type I, fibronectin, and dermal fibroblast function and activity, particularly in the context of systemic sclerosis (SSc)[190]. Furthermore, as previously stated the literature has highlighted the effects of caspase inhibition on collagen production, with studies demonstrating that caspase inhibition can lead to an upregulation of collagen I mRNA[191]. These findings collectively support the potential of NAC in modulating fibronectin and collagen production, providing a basis for further exploration of its therapeutic role in restoring ECM homeostasis.

The findings presented in this study unravel molecular events triggered by CSE in lung fibroblasts, shedding light on the activation of caspase-1, -8, and -3. The study's focus on specific molecular events in response to CSE exposure warrants further investigation into the broader impact of these events on lung tissue homeostasis and disease pathogenesis, particularly in the context of chronic obstructive pulmonary disease. The study's identification of the link between caspase activation and ECM disruption in CSE-exposed lung fibroblasts offers a perspective on the mechanisms driving airway remodeling in the context of cigarette smoke exposure contributing to a more comprehensive understanding of the molecular events triggered by CSE in lung fibroblasts. However, the limitations include the use of cell lines and the need for further validation of the findings in in vivo models and clinical studies to fully elucidate the clinical relevance and therapeutic potential of the observed molecular events in the context of smoking-related lung diseases.

This project entailed the establishment of a collection of primary human lung fibroblasts at RiMed laboratories, obtained from a diverse pool of patients. This endeavour was of significant importance on multiple fronts, representing an advancement in the understanding of molecular and cellular responses in human lung fibroblasts, particularly in the context of

stimuli including cigarette smoke extract. The creation of this unique repository of phLFs not only offered an invaluable resource for scientific inquiry but also addressed critical aspects relevant to the complexities of smoking-related lung diseases. Primarily, the isolation of phLFs from a substantial cohort of patients offers a more clinically relevant model compared to conventional cell lines. This collection enables the exploration of inter-individual variations in cellular responses, a crucial consideration given the diverse genetic and environmental factors that contribute to the spectrum of smoking-related lung diseases. The heterogeneity within this collection facilitates a nuanced investigation into the molecular and cellular intricacies that underscore the pathogenesis of these diseases, allowing for a more personalized and targeted approach to therapeutic interventions. The foundational importance of initiating a repository of patient-derived human lung fibroblasts stems from the indispensable role these cells play in both lung health and disease. Lung fibroblasts are instrumental in maintaining the structural integrity of the alveoli, participating in proliferation, and contributing to the repair of injured lung areas. In the specific context of idiopathic pulmonary fibrosis (IPF), fibroblasts assume a central role in the pathogenesis, exhibiting exaggerated and abnormal responses. Thus, the establishment of this collection of patient-derived human lung fibroblasts becomes a linchpin in comprehending the behavior of these cells in various lung conditions. Within this diverse collection, emphasis was placed on the acquisition of lung fibroblasts from a control group comprising no-smoker patients with normal lung function. Lung fibroblasts from no-COPD and no-smoker patients are inherently limited in availability, as surgical resections related to lung conditions often involve individuals with a history of smoking or COPD. The procurement of N=10 fibroblasts from this subset presented a unique research opportunity, untethered from the confounding factors of smoking or COPD, both recognized as influential determinants of lung fibroblast function and behavior [192,193]. The significance of this subset within the collection becomes evident in the realm of comparative studies, providing a controlled environment to contrast with fibroblasts sourced from individuals with a history of smoking or COPD [194].

The third aim of the study had the purpose to evaluate cleaved GSDMD and cleaved caspase-3 in lung parenchyma tissue sections through immunohistochemistry. However, the evaluation of lung fibroblasts using this technique faced challenges in this particular tissue area. Lung fibroblasts were not well-dispersed, making it difficult to accurately mark them with

the chosen methodology. Previous findings indicated a higher expression of GSDMD in macrophages compared to lung fibroblasts. Additionally, results from the initial phase of the project revealed that GSDMD remained inactive in lung fibroblasts even after exposure to cigarette smoke extract (CSE) stimulation. Consequently, the research focus shifted towards macrophages, recognizing them as pivotal immune cells implicated in the inflammatory response to cigarette smoke exposure. An obstacle encountered during the research was the unavailability of the Cleaved-GSDME antibody at that time. As an alternative, Cleaved-caspase-3 was selected as a surrogate marker for GSDME activation. The decision was made considering its role as executioner of GSDME. The observed higher expression of the two target proteins in macrophages compared to fibroblasts is attributed to the distinct functions of these cell types within the lung environment. Macrophages play a crucial role in the inflammatory response, and their abundance in the tissue area further supported the decision to focus on them for a more comprehensive understanding of the effects of cigarette smoke exposure.

The observed increase in cleaved gasdermin D in lung macrophages from smokers, as compared to ex-smokers or non-smoking controls, constitutes a critical insight into the intricate molecular landscape of cigarette smoke-associated lung diseases. Despite the constraint of a limited patient pool, the presented data strongly support the notion that GSDMD cleavage is increased by cigarette smoking, potentially playing a contributory role in the pathogenesis of CS-associated lung diseases. This discovery acquires even greater significance with the identification of increased GSDMD cleavage specifically in the lungs of smokers, emphasizing the potential pathophysiological relevance of these mechanisms in the context of smoking-related lung diseases. The increased cleavage of GSDMD in lung macrophages from smokers suggests a role for GSDMD as a potential therapeutic target in smoking-associated lung diseases. This revelation forms a solid foundation for further research endeavors aimed at developing targeted interventions that could mitigate the impact of GSDMD cleavage in the landscape of smoking-induced lung pathologies. The identification of GSDMD as a potential player in the pathogenesis of smoking-related lung diseases opens up a new avenue for therapeutic exploration, potentially allowing for the development of innovative strategies to intervene in the progression of these debilitating conditions. Furthermore, the increase of cleaved caspase-3 in alveolar macrophages within a subset of

lung tissue sections from smoking subjects, as opposed to no-smoker controls, underscore that the alveolar macrophages of smokers exhibit features indicative of dysregulated cell death. These discoveries were published in two journals in 2022 [81] and 2023 [158]. The results obtained, supported by literature[195], have led to the hypothesis of a role for cleaved GSDMD as a biomarker of chronic inflammation.

The hypothesis was presented within the framework of the CA20117 project Converting molecular profiles of myeloid cells into biomarkers for inflammation and cancer (Mye-InfoBank) aiming at identifying novel markers of myeloid cells for DACI.

In particular, during the Short-Term Scientific Mission (STSM), preliminary results emerged, cleaved GSDMD revealed intensified staining in macrophages within both colorectal and lung cancer tissues compared to non-tumor-adjacent counterparts. These initial findings hint at the potential involvement of GSDMD cleavage also in cancer progression, suggesting an active inflammasome in the lung tumor microenvironment. The implications extend beyond lung cancer to colorectal cancer, opening up a novel perspective on the role of GSDMD in cancer-related inflammation. The upregulation of GSDMD in human non-small cell lung cancer tissue, coupled with its association with tumor size and TNM stages, underscores the multifaceted role of GSDMD in promoting lung cancer growth. The identified increase in GSDMD cleavage in lung macrophages of smokers not only expands our understanding of the pathophysiological relevance of these mechanisms but also suggests potential therapeutic avenues. The heightened cleavage of GSDMD in smokers' lungs and its potential role as a therapeutic target in lung cancer highlight the complexity of molecular events triggered by cigarette smoking. The identification of dysregulated cell death features in alveolar macrophages of smokers further underscores the need for a comprehensive exploration of these mechanisms in smoking-related lung diseases, particularly COPD. Preliminary results from the STSM not only provide insights into the potential role of GSDMD in cancer progression but also shed light on its association with inflammasome activity in the tumor microenvironment. These collective findings underscore the need for continued research in this area to fully elucidate the roles of GSDMD and caspase-3 in smoking-related conditions and to explore their potential as therapeutic targets.

Conclusion

The results obtained during the present PhD project have contributed to a better understanding of the molecular changes associated with cigarette smoke exposure in lung fibroblasts. The investigation of inflammasome-dependent responses in human lung fibroblasts uncovered a complex interplay involving caspase-1, -8, and -3 activation triggered by cigarette smoke extract. While activation of the NLRP3 inflammasome was ruled out, the study revealed the participation of the molecular axis involving caspase-8, caspase-3/7, and gasdermin E. This research enlightened an association between caspase activation and extracellular matrix disruption in lung fibroblasts exposed to cigarette smoke extract providing insights into the mechanisms influencing airway remodeling (Fig.22).

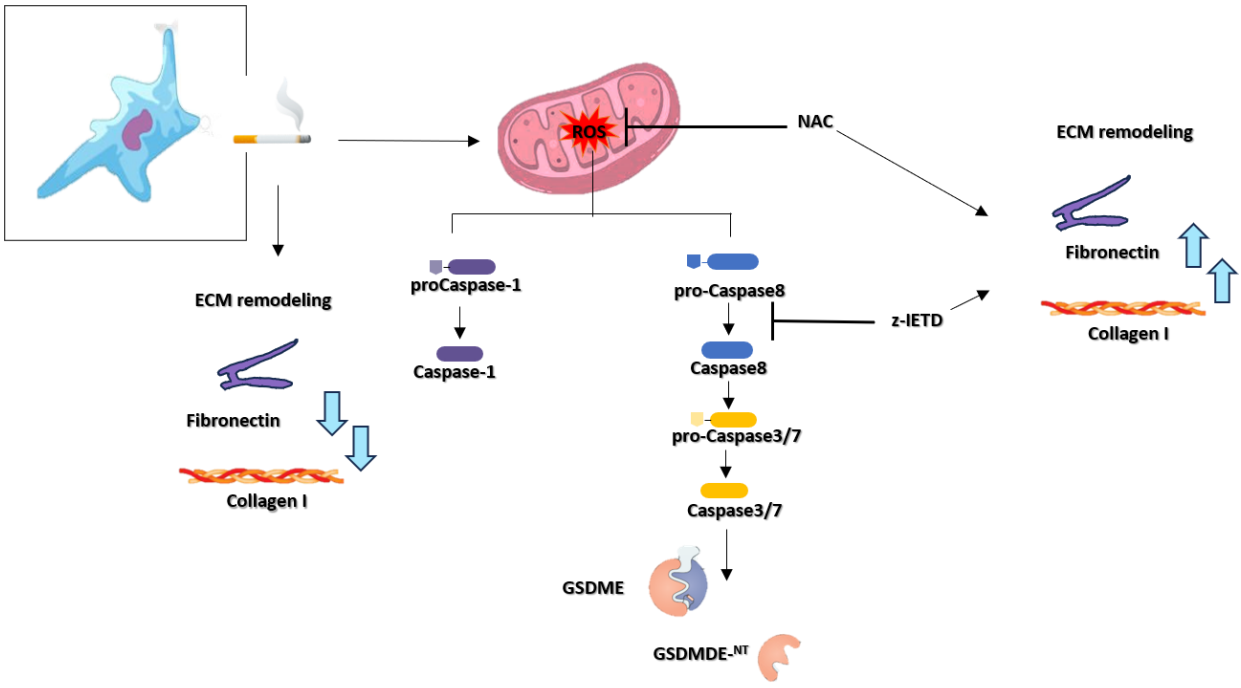

Fig.22: Graphical abstract of the main findings in human lung fibroblasts. *Upon exposure to cigarette smoke extract, activation of caspase-1, -8 and -3/7 was observed. Caspase-3/7 activation was identified to be caspase-8 dependent. N-acetylcysteine (NAC), antioxidant and cytoprotectant, not only inhibited all caspase activities but also mitigated reactive oxygen species in the mitochondria. This linked caspase activation directly with oxidative stress and mitochondrial damage. Inhibition of Caspase-8 prevented GSDME cleavage, establishing the axis caspase-8 – caspase 3/7 – GSDME-NT as activated in response to CSE. CSE exposure induced a decrease in Collagen-I and fibronectin release, and treatments with z-IETD (caspase-8 inhibitor) and NAC effectively restored ECM homeostasis. These findings underscored the*

critical role of caspase-8-caspase-3/7 activation in ECM disruption in human lung fibroblasts treated with cigarette smoke.

This contributes to a more holistic understanding of the molecular events initiated by cigarette smoke exposure in lung fibroblasts. The establishment of a collection of primary human lung fibroblasts from smokers, ex-smokers and no-smokers provided a resource for exploring inter-individual variations in cellular responses. The investigation into cleaved GSDMD and caspase-3 in tissue sections not only implicated GSDMD in the pathogenesis of smoking-related lung diseases but also hinted at its potential role in cancer-related inflammation, particularly in lung and colorectal cancer. These findings offer avenues for therapeutic exploration and emphasizing the need for further research into the roles of GSDMD and caspase-3 in smoking-related conditions and cancer progression. While acknowledging the limitations, such as the use of cell lines and the necessity for validation of in vivo models and clinical studies, this study represents a significant step forward in unraveling the complexities of smoking-induced cellular responses in lung fibroblasts.

References

1. Adeloye, D. *et al.* Global, regional, and national prevalence of, and risk factors for, chronic obstructive pulmonary disease (COPD) in 2019: a systematic review and modelling analysis. *Lancet Respir Med* **10**, 447–458 (2022).
2. Greenlund, K. J., Liu, Y., Deokar, A. J., Wheaton, A. G. & Croft, J. B. Association of chronic obstructive pulmonary disease with increased confusion or memory loss and functional limitations among adults in 21 states, 2011 behavioral risk factor surveillance system. *Prev Chronic Dis* **13**, (2023).
3. Antó, J. M., Vermeire, P., Vestbo, J. & Sunyer, J. Epidemiology of chronic obstructive pulmonary disease. *European Respiratory Journal* **17**, 982–994 (2001).
4. Chronic Obstructive Pulmonary Disease (COPD) | CDC. https://www.cdc.gov/copd/index.html.
5. Petty, T. L. The history of COPD. *Int J Chron Obstruct Pulmon Dis* **1**, 3–14 (2006).
6. Alqahtani, J. S. *et al.* Prevalence, Severity and Mortality associated with COPD and Smoking in patients with COVID-19: A Rapid Systematic Review and Meta-Analysis. *PLoS One* **15**, (2020).
7. Aghapour, M., Raee, P., Moghaddam, S. J., Hiemstra, P. S. & Heijink, I. H. Airway epithelial barrier dysfunction in chronic obstructive pulmonary disease: Role of cigarette smoke exposure. *Am J Respir Cell Mol Biol* **58**, 157–169 (2018).
8. What's In a Cigarette? | American Lung Association. https://www.lung.org/quit-smoking/smoking-facts/whats-in-a-cigarette.

9. Ferraro, M. *et al.* Budesonide, Aclidinium and Formoterol in combination limit inflammaging processes in bronchial epithelial cells exposed to cigarette smoke. *Exp Gerontol* **118**, 78–87 (2019).

10. Hou, W. *et al.* Cigarette Smoke Induced Lung Barrier Dysfunction, EMT, and Tissue Remodeling: A Possible Link between COPD and Lung Cancer. *Biomed Res Int* **2019**, (2019).

11. Wong, M. H. & Johnson, M. D. Differential Response of Primary Alveolar Type I and Type II Cells to LPS Stimulation. *PLoS One* **8**, (2013).

12. Chaplin, D. D. Overview of the Immune Response. *J Allergy Clin Immunol* **125**, S3 (2010).

13. Fu, Y. S. *et al.* Polyphenols, flavonoids and inflammasomes: the role of cigarette smoke in COPD. *European Respiratory Review* **31**, (2022).

14. Nurwidya, F., Damayanti, T. & Yunus, F. The Role of Innate and Adaptive Immune Cells in the Immunopathogenesis of Chronic Obstructive Pulmonary Disease. *Tuberc Respir Dis (Seoul)* **79**, 5 (2016).

15. Lin, L., Li, J., Song, Q., Cheng, W. & Chen, P. The role of HMGB1/RAGE/TLR4 signaling pathways in cigarette smoke-induced inflammation in chronic obstructive pulmonary disease. *Immun Inflamm Dis* **10**, e711 (2022).

16. Metcalfe, H. J. *et al.* Effects of cigarette smoke on Toll-like receptor (TLR) activation of chronic obstructive pulmonary disease (COPD) macrophages. *Clin Exp Immunol* **176**, 461 (2014).

17. Bissonnette, E. Y., Lauzon-Joset, J. F., Debley, J. S. & Ziegler, S. F. Cross-Talk Between Alveolar Macrophages and Lung Epithelial Cells is Essential to Maintain Lung Homeostasis. *Front Immunol* **11**, (2020).

18. Wu, Y. *et al.* The role of the NLRP3 inflammasome in chronic inflammation in asthma and chronic obstructive pulmonary disease. *Immun Inflamm Dis* **10**, (2022).

19. Leszczyńska, K., Jakubczyk, D. & Górska, S. The NLRP3 inflammasome as a new target in respiratory disorders treatment. *Front Immunol* **13**, (2022).

20. Kelley, N., Jeltema, D., Duan, Y. & He, Y. The NLRP3 Inflammasome: An Overview of Mechanisms of Activation and Regulation. *Int J Mol Sci* **20**, (2019).

21. Pouwels, S. D. *et al.* DAMPs activating innate and adaptive immune responses in COPD. *Mucosal Immunol* **7**, 215–226 (2014).

22. Swanson, K. V., Deng, M. & Ting, J. P. Y. The NLRP3 inflammasome: molecular activation and regulation to therapeutics. *Nat Rev Immunol* **19**, 477 (2019).

23. Huang, Y., Xu, W. & Zhou, R. NLRP3 inflammasome activation and cell death. *Cell Mol Immunol* **18**, 2114 (2021).

24. Wang, C. *et al.* NLRP3 inflammasome activation triggers gasdermin D-independent inflammation. *Sci Immunol* **6**, eabj3859 (2021).

25. He, W. T. *et al.* Gasdermin D is an executor of pyroptosis and required for interleukin-1β secretion. *Cell Research 2015 25:12* **25**, 1285–1298 (2015).

26. Phulphagar, K. *et al.* Proteomics reveals distinct mechanisms regulating the release of cytokines and alarmins during pyroptosis. *Cell Rep* **34**, (2021).

27. Blevins, H. M., Xu, Y., Biby, S. & Zhang, S. The NLRP3 Inflammasome Pathway: A Review of Mechanisms and Inhibitors for the Treatment of Inflammatory Diseases. *Front Aging Neurosci* **14**, (2022).

28. Zhang, J. *et al.* New Insights into the Role of NLRP3 Inflammasome in Pathogenesis and Treatment of Chronic Obstructive Pulmonary Disease. *J Inflamm Res* **14**, 4155 (2021).

29. Franchi, L., Eigenbrod, T., Muñoz-Planillo, R. & Nuñez, G. The inflammasome: A caspase-1-activation platform that regulates immune responses and disease pathogenesis. *Nature Immunology* vol. 10 241–247 Preprint at https://doi.org/10.1038/ni.1703 (2009).

30. Pinkerton, J. W. *et al.* Inflammasomes in the lung. *Mol Immunol* **86**, 44–55 (2017).

31. Faner, R. *et al.* The inflammasome pathway in stable COPD and acute exacerbations. *ERJ Open Res* **2**, (2016).

32. Pinkerton, J. W. *et al.* Inflammasomes in the lung. *Mol Immunol* **86**, 44–55 (2017).

33. Li, C. *et al.* The Nucleotide-Binding Oligomerization Domain-Like Receptor Family Pyrin Domain-Containing 3 Inflammasome Regulates Bronchial Epithelial Cell Injury and Proapoptosis after Exposure to Biomass Fuel Smoke. *Am J Respir Cell Mol Biol* **55**, 815–824 (2016).

34. Yi, G. *et al.* A large lung gene expression study identifying IL1B as a novel player in airway inflammation in COPD airway epithelial cells. *Inflamm Res* **67**, 539–551 (2018).

35. Kang, M. J. *et al.* Suppression of NLRX1 in chronic obstructive pulmonary disease. *J Clin Invest* **125**, 2458–2462 (2015).

36. Birrell, M. A., Wong, S., Catley, M. C. & Belvisi, M. G. Impact of tobacco-smoke on key signaling pathways in the innate immune response in lung macrophages. *J Cell Physiol* **214**, 27–37 (2008).

37. Han, S. H., Jerome, J. A., Gregory, A. D. & Mallampalli, R. K. Cigarette smoke destabilizes NLRP3 protein by promoting its ubiquitination. *Respir Res* **18**, (2017).

38. Buscetta, M. *et al.* Cigarette smoke inhibits the NLRP3 inflammasome and leads to caspase-1 activation via the TLR4-TRIF-caspase-8 axis in human macrophages. *The FASEB Journal* **34**, 1819–1832 (2020).

39. Kesavardhana, S., Malireddi, R. K. S. & Kanneganti, T. D. Caspases in Cell Death, Inflammation, and Pyroptosis. *https://doi.org/10.1146/annurev-immunol-073119-095439* **38**, 567–595 (2020).

40. Svandova, E., Lesot, H., Sharpe, P. & Matalova, E. Making the head: Caspases in life and death. *Front Cell Dev Biol* **10**, 1075751 (2023).

41. Pérez-Garijo, A. When dying is not the end: Apoptotic caspases as drivers of proliferation. *Semin Cell Dev Biol* **82**, 86–95 (2018).

42. Nakajima, Y. I. & Kuranaga, E. Caspase-dependent non-apoptotic processes in development. *Cell Death & Differentiation 2017 24:8* **24**, 1422–1430 (2017).

43. Jan, R. & Chaudhry, G. e. S. Understanding Apoptosis and Apoptotic Pathways Targeted Cancer Therapeutics. *Adv Pharm Bull* **9**, 205 (2019).

44. Elmore, S. Apoptosis: A Review of Programmed Cell Death. *Toxicol Pathol* **35**, 495 (2007).

45. Boice, A. & Bouchier-Hayes, L. Targeting apoptotic caspases in cancer. *Biochimica et Biophysica Acta (BBA) - Molecular Cell Research* **1867**, 118688 (2020).

46. Weinlich Brunner G P Amarante-Mendes, R. T., Weinlich P Amarante-Mendes, R. G. & Brunner, T. Control of death receptor ligand activity by posttranslational modifications. doi:10.1007/s0oo18-01O-0289-7.

47. Brentnall, M., Rodriguez-Menocal, L., De Guevara, R. L., Cepero, E. & Boise, L. H. Caspase-9, caspase-3 and caspase-7 have distinct roles during intrinsic apoptosis. *BMC Cell Biol* **14**, 1–9 (2013).

48. Chipuk, J. E., Bouchier-Hayes, L. & Green, D. R. Mitochondrial outer membrane permeabilization during apoptosis: the innocent bystander scenario. *Cell Death & Differentiation 2006 13:8* **13**, 1396–1402 (2006).

49. Bender, T. & Martinou, J. C. Where Killers Meet—Permeabilization of the Outer Mitochondrial Membrane during Apoptosis. *Cold Spring Harb Perspect Biol* **5**, (2013).

50. Vringer, E. & Tait, S. W. G. Mitochondria and cell death-associated inflammation. *Cell Death & Differentiation 2022 30:2* **30**, 304–312 (2022).

51. Bender, T. & Martinou, J. C. Where Killers Meet—Permeabilization of the Outer Mitochondrial Membrane during Apoptosis. *Cold Spring Harb Perspect Biol* **5**, (2013).

52. Tait, S. W. G. & Green, D. R. Mitochondria and cell death: outer membrane permeabilization and beyond. *Nature Reviews Molecular Cell Biology 2010 11:9* **11**, 621–632 (2010).

53. Heilig, R. *et al.* Caspase-1 cleaves Bid to release mitochondrial SMAC and drive secondary necrosis in the absence of GSDMD. *Life Sci Alliance* **3**, (2020).

54. Orning, P. & Lien, E. Multiple roles of caspase-8 in cell death, inflammation, and innate immunity. *J Leukoc Biol* **109**, 121–141 (2021).

55. Redza-Dutordoir, M. & Averill-Bates, D. A. Activation of apoptosis signalling pathways by reactive oxygen species. *Biochimica et Biophysica Acta (BBA) - Molecular Cell Research* **1863**, 2977–2992 (2016).

56. Khosravi-Far, R. & Esposti, M. D. Death Receptor Signals to Mitochondria. *Cancer Biol Ther* **3**, 1051 (2004).

57. Beaudouin, J., Liesche, C., Aschenbrenner, S., Hörner, M. & Eils, R. Caspase-8 cleaves its substrates from the plasma membrane upon CD95-induced apoptosis. *Cell Death & Differentiation 2013 20:4* **20**, 599–610 (2013).

58. McIlwain, D. R., Berger, T. & Mak, T. W. Caspase Functions in Cell Death and Disease. *Cold Spring Harb Perspect Biol* **5**, 1–28 (2013).

59. Annibaldi, A. & Walczak, H. Death Receptors and Their Ligands in Inflammatory Disease and Cancer. *Cold Spring Harb Perspect Biol* **12**, a036384 (2020).

60. Guicciardi, M. E. & Gores, G. J. Life and death by death receptors. *The FASEB Journal* **23**, 1625 (2009).

61. Suhaili, S. H., Karimian, H., Stellato, M., Lee, T. H. & Aguilar, M. I. Mitochondrial outer membrane permeabilization: a focus on the role of mitochondrial membrane structural organization. *Biophys Rev* **9**, 443 (2017).

62. Wei, X. *et al.* Role of pyroptosis in inflammation and cancer. *Cellular & Molecular Immunology 2022 19:9* **19**, 971–992 (2022).

63. Liu, J., Fan, G., Tao, N. & Sun, T. Role of Pyroptosis in Respiratory Diseases and its Therapeutic Potential. *J Inflamm Res* **15**, 2033 (2022).

64. Tang, L., Lu, C., Zheng, G. & Burgering, B. M. T. Emerging insights on the role of gasdermins in infection and inflammatory diseases. *Clin Transl Immunology* **9**, (2020).

65. Chen, S., Jiang, J., Li, T. & Huang, L. PANoptosis: Mechanism and Role in Pulmonary Diseases. *International Journal of Molecular Sciences 2023, Vol. 24, Page 15343* **24**, 15343 (2023).

66. Nowowiejska, J. *et al.* Gasdermin E (GSDME)—A New Potential Marker of Psoriasis and Its Metabolic Complications: The First Combined Study on Human Serum, Urine and Tissue. *Cells* **12**, 2149 (2023).

67. Mulla, J., Katti, R. & Scott, M. J. The Role of Gasdermin-D-Mediated Pryoptosis in Organ Injury and Its Therapeutic Implications. *Organogenesis* **19**, (2023).

68. Lee, E., Song, C. H., Bae, S. J., Ha, K. T. & Karki, R. Regulated cell death pathways and their roles in homeostasis, infection, inflammation, and tumorigenesis. *Experimental & Molecular Medicine 2023 55:8* **55**, 1632–1643 (2023).

69. Liu, X. *et al.* Role of GSDM family members in airway epithelial cells of lung diseases: a systematic and comprehensive transcriptomic analysis. *Cell Biol Toxicol* **1**, 1–18 (2023).

70. Bowie, A. G. Mechanisms of gasdermin pore formation in response to viral sensing in human respiratory epithelial cells. (2023).

71. Liu, X., Xia, S., Zhang, Z., Wu, H. & Lieberman, J. Channelling inflammation: gasdermins in physiology and disease. *Nature Reviews Drug Discovery 2021 20:5* **20**, 384–405 (2021).

72. Broz, P., Pelegrín, P. & Shao, F. The gasdermins, a protein family executing cell death and inflammation. *Nature Reviews Immunology 2019 20:3* **20**, 143–157 (2019).

73. Dai, Z. *et al.* Gasdermin D-mediated pyroptosis: mechanisms, diseases, and inhibitors. *Front Immunol* **14**, (2023).

74. Mulla, J., Katti, R. & Scott, M. J. The Role of Gasdermin-D-Mediated Pyroptosis in Organ Injury and Its Therapeutic Implications. *Organogenesis* **19**, (2023).

75. Shao, R. *et al.* Review: the role of GSDMD in sepsis. *Inflammation Research* **71**, 1191–1202 (2022).

76. Liu, X. *et al.* Inflammasome-activated gasdermin D causes pyroptosis by forming membrane pores. *Natur* **535**, 153–158 (2016).

77. Tang, L., Lu, C., Zheng, G. & Burgering, B. M. T. Emerging insights on the role of gasdermins in infection and inflammatory diseases. *Clin Transl Immunology* **9**, e1186 (2020).

78. Sikkema, L. *et al.* An integrated cell atlas of the lung in health and disease. *Nat Med* **29**, 1563–1577 (2023).

79. Huot-Marchand, S. *et al.* Cigarette smoke-induced gasdermin D activation in bronchoalveolar macrophages and bronchial epithelial cells dependently on NLRP3. *Front Immunol* **13**, 918507 (2022).

80. Liu, J., Fan, G., Tao, N. & Sun, T. Role of Pyroptosis in Respiratory Diseases and its Therapeutic Potential. *J Inflamm Res* **15**, 2033 (2022).

81. Buscetta, M. *et al.* Cigarette smoke promotes inflammasome-independent activation of caspase-1 and -4 leading to gasdermin D cleavage in human macrophages. *The FASEB Journal* **36**, e22525 (2022).

82. Liu, X., Huang, X. & Xu, F. The influence of pyroptosis-related genes on the development of chronic obstructive pulmonary disease. *BMC Pulm Med* **23**, 1–12 (2023).

83. Xia, S., Hollingsworth, L. R. & Wu, H. Mechanism and Regulation of Gasdermin-Mediated Cell Death. *Cold Spring Harb Perspect Biol* **12**, (2020).

84. Tan, G., Huang, C., Chen, J., Chen, B. & Zhi, F. Gasdermin-E-mediated pyroptosis participates in the pathogenesis of Crohn's disease by promoting intestinal inflammation. *Cell Rep* **35**, 109265 (2021).

85. Tan, G., Huang, C., Chen, J. & Zhi, F. HMGB1 released from GSDME-mediated pyroptotic epithelial cells participates in the tumorigenesis of colitis-associated colorectal cancer through the ERK1/2 pathway. *J Hematol Oncol* **13**, 1–11 (2020).

86. Zhang, Z. *et al.* Prognostic and Immunological Role of Gasdermin E in Pan-Cancer Analysis. *Front Oncol* **11**, (2021).

87. Rogers, C. *et al.* Gasdermin pores permeabilize mitochondria to augment caspase-3 activation during apoptosis and inflammasome activation. *Nat Commun* **10**, (2019).

88. Rogers, C. *et al.* Cleavage of DFNA5 by caspase-3 during apoptosis mediates progression to secondary necrotic/pyroptotic cell death. *Nature Communications 2017 8:1* **8**, 1–14 (2017).

89. Gong, W. *et al.* Intestinal Gasdermins for regulation of inflammation and tumorigenesis. *Front Immunol* **13**, 1052111 (2022).

90. Orning, P., Lien, E. & Fitzgerald, K. A. Gasdermins and their role in immunity and inflammation. *Journal of Experimental Medicine* **216**, 2453–2465 (2019).

91. Li, Y. *et al.* GSDME-mediated pyroptosis promotes inflammation and fibrosis in obstructive nephropathy. *Cell Death Differ* **28**, 2333–2350 (2021).

92. Wu, M. *et al.* Gasdermin E Deletion Attenuates Ureteral Obstruction- and 5/6 Nephrectomy-Induced Renal Fibrosis and Kidney Dysfunction. *Front Cell Dev Biol* **9**, 2993 (2021).

93. Song, Z., Gong, Q. & Guo, J. Pyroptosis: Mechanisms and Links with Fibrosis. *Cells 2021, Vol. 10, Page 3509* **10**, 3509 (2021).

94. Yang, H. *et al.* Pyroptosis executor gasdermin D plays a key role in scleroderma and bleomycin-induced skin fibrosis. *Cell Death Discov* **8**, (2022).

95. Song, M. *et al.* Inhibition of gasdermin D-dependent pyroptosis attenuates the progression of silica-induced pulmonary inflammation and fibrosis. *Acta Pharm Sin B* **12**, 1213–1224 (2022).

96. Broz, P. & Dixit, V. M. Inflammasomes: mechanism of assembly, regulation and signalling. *Nature Reviews Immunology 2016 16:7* **16**, 407–420 (2016).

97. Hewitt, R. J. & Lloyd, C. M. Regulation of immune responses by the airway epithelial cell landscape. *Nature Reviews Immunology 2021 21:6* **21**, 347–362 (2021).

98. Thiam, F. *et al.* Understanding fibroblast-immune cell interactions via co-culture models and their role in asthma pathogenesis. *Front Immunol* **14**, 1128023 (2023).

99. Burgoyne, R. A., Fisher, A. J. & Borthwick, L. A. The Role of Epithelial Damage in the Pulmonary Immune Response. *Cells* **10**, (2021).

100. Colarusso, C., Terlizzi, M., Molino, A., Pinto, A. & Sorrentino, R. Role of the inflammasome in chronic obstructive pulmonary disease (COPD). *Oncotarget* **8**, 81813 (2017).

101. Holz, O. *et al.* Lung fibroblasts from patients with emphysema show a reduced proliferation rate in culture. *European Respiratory Journal* **24**, 575–579 (2004).

102. Woldhuis, R. R. *et al.* COPD-derived fibroblasts secrete higher levels of senescence-associated secretory phenotype proteins. *Thorax* **76**, 508–511 (2021).

103. Basma, H. *et al.* Reprogramming of COPD lung fibroblasts through formation of induced pluripotent stem cells. *Am J Physiol Lung Cell Mol Physiol* **306**, 552–565 (2014).

104. Togo, S. *et al.* Lung Fibroblast Repair Functions in Patients with Chronic Obstructive Pulmonary Disease Are Altered by Multiple Mechanisms. *Am J Respir Crit Care Med* **178**, 248 (2008).

105. Júnior, C. *et al.* Multi-Step Extracellular Matrix Remodelling and Stiffening in the Development of Idiopathic Pulmonary Fibrosis. *Int J Mol Sci* **24**, (2023).

106. White, E. S. Lung extracellular matrix and fibroblast function. *Ann Am Thorac Soc* **12**, S30–S33 (2015).

107. Hackett, T. L. & Osei, E. T. Modeling Extracellular Matrix-Cell Interactions in Lung Repair and Chronic Disease. *Cells* **10**, 2145 (2021).

108. Burgstaller, G. *et al.* The instructive extracellular matrix of the lung: basic composition and alterations in chronic lung disease. *European Respiratory Journal* **50**, 1601805 (2017).

109. Y, A. *et al.* Fibronectin production by cultured human lung fibroblasts in three-dimensional collagen gel culture. *In Vitro Cell Dev Biol Anim* **34**, 203–210 (1998).

110. Bradbury, P. *et al.* Tropomyosin 2.1 collaborates with fibronectin to promote TGF-β1-induced contraction of human lung fibroblasts. *Respir Res* **22**, 1–10 (2021).

111. Kolb, M. *et al.* Transient Transgene Expression of Decorin in the Lung Reduces the Fibrotic Response to Bleomycin. *https://doi.org/10.1164/ajrccm.163.3.2006084* **163**, 770–777 (2012).

112. White, E. S. Lung extracellular matrix and fibroblast function. *Ann Am Thorac Soc* **12**, S30–S33 (2015).

113. Zhan, J.-H. *et al.* Investigation of a UPR-Related Gene Signature Identifies the Pro-Fibrotic Effects of Thrombospondin-1 by Activating CD47/ROS/Endoplasmic Reticulum Stress Pathway in Lung Fibroblasts. *Antioxidants 2023, Vol. 12, Page 2024* **12**, 2024 (2023).

114. Hu, X., Jiang, C., Hu, N. & Hong, S. ADAMTS1 induces epithelial-mesenchymal transition pathway in non-small cell lung cancer by regulating TGF-β. *Aging* **15**, 2097–2114 (2023).

115. Zhou, Y. *et al.* Extracellular Matrix in Lung Development, Homeostasis and Disease. *Matrix Biol* **73**, 77 (2018).

116. Ito, J. T. *et al.* Extracellular Matrix Component Remodeling in Respiratory Diseases: What Has Been Found in Clinical and Experimental Studies? *Cells 2019, Vol. 8, Page 342* **8**, 342 (2019).

117. Van Linthout, S., Miteva, K. & Tschöpe, C. Crosstalk between fibroblasts and inflammatory cells. *Cardiovasc Res* **102**, 258–269 (2014).

118. Li, R., Wen, A. & Lin, J. Pro-Inflammatory Cytokines in the Formation of the Pre-Metastatic Niche. *Cancers (Basel)* **12**, 1–16 (2020).

119. Yap, J. M. G. *et al.* Human Lung Fibroblasts Exhibit Induced Inflammation Memory via Increased IL6 Gene Expression and Release. *Front Immunol* **13**, 1 (2022).

120. Ghonim, M. A., Boyd, D. F., Flerlage, T. & Thomas, P. G. Pulmonary inflammation and fibroblast immunoregulation: from bench to bedside. *J Clin Invest* **133**, (2023).

121. Nakano, R. *et al.* Non-Transcriptional and Translational Function of Canonical NF-κB Signaling in Activating ERK1/2 in IL-1β-Induced COX-2 Expression in Synovial Fibroblasts. *Front Immunol* **11**, 579266 (2020).

122. Xu, L. *et al.* Interleukin-29 induces receptor activator of NF-κB ligand expression in fibroblast-like synoviocytes via MAPK signaling pathways. *Int J Rheum Dis* **18**, 842–849 (2015).

123. Su, X., Wu, W., Zhu, Z., Lin, X. & Zeng, Y. The effects of epithelial–mesenchymal transitions in COPD induced by cigarette smoke: an update. *Respiratory Research 2022 23:1* **23**, 1–18 (2022).

124. Eapen, M. S. *et al.* Increased myofibroblasts in the small airways, and relationship to remodelling and functional changes in smokers and COPD patients: potential role of epithelial-mesenchymal transition. *ERJ Open Res* **7**, (2021).

125. Molla, M. D. *et al.* Role of Caspase-1 in the Pathogenesis of Inflammatory-Associated Chronic Noncommunicable Diseases. *J Inflamm Res* **13**, 749 (2020).

126. Kawaguchi, M. *et al.* Inflammasome Activation of Cardiac Fibroblasts Is Essential for Myocardial Ischemia/Reperfusion Injury. *Circulation* **123**, 594–604 (2011).

127. Artlett, C. M. *et al.* The inflammasome activating caspase 1 mediates fibrosis and myofibroblast differentiation in systemic sclerosis. *Arthritis Rheum* **63**, 3563–3574 (2011).

128. Tezcan, G. *et al.* Therapeutic Potential of Pharmacological Targeting NLRP3 Inflammasome Complex in Cancer. *Front Immunol* **11**, (2021).

129. Fu, Y. *et al.* Polydatin relieves paraquat-induced human MRC-5 fibroblast injury through inhibiting the activation of the NLRP3 inflammasome. *Ann Transl Med* **8**, 765–765 (2020).

130. Effendi, W. I. & Nagano, T. The Crucial Role of NLRP3 Inflammasome in Viral Infection-Associated Fibrosing Interstitial Lung Diseases. *Int J Mol Sci* **22**, (2021).

131. Kelly, P., Meade, K. G. & O'Farrelly, C. Non-canonical inflammasome-mediated IL-1β production by primary endometrial epithelial and stromal fibroblast cells is NLRP3 and caspase-4 dependent. *Front Immunol* **10**, 430475 (2019).

132. Hou, H. H., Pan, H. J., Liao, W. Y., Lee, C. H. & Yu, C. J. Autophagy in fibroblasts induced by cigarette smoke extract promotes invasion in lung cancer cells. *Int J Cancer* **147**, 2587–2596 (2020).

133. Ershaid, N. *et al.* NLRP3 inflammasome in fibroblasts links tissue damage with inflammation in breast cancer progression and metastasis. *Nature Communications 2019 10:1* **10**, 1–15 (2019).

134. Shao, H., Yi, X. M. & Wells, A. Epidermal growth factor protects fibroblasts from apoptosis via PI3 kinase and Rac signaling pathways. *Wound Repair Regen* **16**, 551–558 (2008).

135. Peeters, P. M., Wouters, E. F. & Reynaert, N. L. Immune homeostasis in epithelial cells: Evidence and role of inflammasome signaling reviewed. *J Immunol Res* **2015**, (2015).

136. Froidure, A., Ladjemi, M. Z. & Pilette, C. Interleukin-1α: a key player for epithelial-to-mesenchymal signalling in COPD? *European Respiratory Journal* **48**, 301–304 (2016).

137. Krimmer, D., Ichimaru, Y., Burgess, J., Black, J. & Oliver, B. Exposure to Biomass Smoke Extract Enhances Fibronectin Release from Fibroblasts. *PLoS One* **8**, e83938 (2013).

138. Song, M. *et al.* Cigarette Smoke Extract Promotes Human Lung Myofibroblast Differentiation by the Induction of Endoplasmic Reticulum Stress. *Respiration* **98**, 347–356 (2019).

139. Hinz, B., Dugina, V., Ballestrem, C., Wehrle-Haller, B. & Chaponnier, C. α-Smooth Muscle Actin Is Crucial for Focal Adhesion Maturation in Myofibroblasts. *Mol Biol Cell* **14**, 2508 (2003).

140. Ahmed, A. *et al.* Caspase 3 activity in isolated fetal rat lung fibroblasts and rat periodontal ligament fibroblasts: cigarette smoke induced alterations. *Tob Induc Dis* **11**, (2013).

141. Drakopanagiotakis, F., Xifteri, A., Polychronopoulos, V. & Bouros, D. Apoptosis in lung injury and fibrosis. *European Respiratory Journal* **32**, 1631–1638 (2008).

142. Nyunoya, T. *et al.* Cigarette Smoke Induces Cellular Senescence. *Am J Respir Cell Mol Biol* **35**, 681 (2006).

143. Murata, K., Fujita, N. & Takahashi, R. Ninjinyoeito ameliorated cigarette smoke extract-induced apoptosis and inflammation through JNK signaling inhibition in human lung fibroblasts. *BMC Complement Med Ther* **22**, 1–10 (2022).

144. Nyunoya, T. *et al.* Cigarette Smoke Induces Cellular Senescence. *Am J Respir Cell Mol Biol* **35**, 681 (2006).

145. Miglino, N. *et al.* Cigarette smoke inhibits lung fibroblast proliferation by translational mechanisms. *European Respiratory Journal* **39**, 705–711 (2012).

146. Kaur, G., Muthumalage, T. & Rahman, I. Clearance of senescent cells reverts the cigarette smoke-induced lung senescence and airspace enlargement in p16-3MR mice. *Aging Cell* **22**, e13850 (2023).

147. Carnevali, S. *et al.* Cigarette smoke extract induces oxidative stress and apoptosis in human lung fibroblasts. *Am J Physiol Lung Cell Mol Physiol* **284**, (2003).

148. Zhang, Y. *et al.* SIRT1 prevents cigarette smoking-induced lung fibroblasts activation by regulating mitochondrial oxidative stress and lipid metabolism. *J Transl Med* **20**, 1–13 (2022).

149. Noordhoek, J. A. *et al.* Different Modulation of Decorin Production by Lung Fibroblasts from Patients with Mild and Severe Emphysema. *COPD: Journal of Chronic Obstructive Pulmonary Disease* **2**, 17–25 (2005).

150. Jaccard, G. *et al.* Mainstream smoke constituents and in vitro toxicity comparative analysis of 3R4F and 1R6F reference cigarettes. *Toxicol Rep* **6**, 222–231 (2019).

151. Kim, Y.-H. *et al.* Comparison of volatile organic compounds between cigarette smoke condensate (CSC) and extract (CSE) samples. *Environ Health Toxicol* **33**, e2018012-0 (2018).

152. O'Brien, M. *et al.* A bioluminescent caspase-1 activity assay rapidly monitors inflammasome activation in cells. *J Immunol Methods* **447**, (2017).

153. Bayir, H. & Kagan, V. E. Bench-to-bedside review: Mitochondrial injury, oxidative stress and apoptosis - There is nothing more practical than a good theory. *Crit Care* **12**, 1–11 (2008).

154. Ott, M., Gogvadze, V., Orrenius, S. & Zhivotovsky, B. Mitochondria, oxidative stress and cell death. *Apoptosis* **12**, 913–922 (2007).

155. Ramos-Ibeas, P., Barandalla, M., Colleoni, S. & Lazzari, G. Pyruvate antioxidant roles in human fibroblasts and embryonic stem cells. *Mol Cell Biochem* **429**, 137–150 (2017).

156. Huot-Marchand, S. *et al.* Cigarette smoke-induced gasdermin D activation in bronchoalveolar macrophages and bronchial epithelial cells dependently on NLRP3. *Front Immunol* **13**, (2022).

157. Huot-Marchand, S. *et al.* Cigarette smoke-induced gasdermin D activation in bronchoalveolar macrophages and bronchial epithelial cells dependently on NLRP3. *Front Immunol* **13**, 918507 (2022).

158. Cristaldi, M. *et al.* Caspase-8 activation by cigarette smoke induces pro-inflammatory cell death of human macrophages exposed to lipopolysaccharide. *Cell Death & Disease 2023 14:11* **14**, 1–11 (2023).

159. Li, Y. *et al.* GSDME-mediated pyroptosis promotes inflammation and fibrosis in obstructive nephropathy. *Cell Death Differ* **28**, 2333–2350 (2021).

160. Bellou, V., Belbasis, L. & Evangelou, E. Tobacco Smoking and Risk for Pulmonary Fibrosis: A Prospective Cohort Study From the UK Biobank. *Chest* **160**, 983–993 (2021).

161. Zhang, W. J., Chen, S. J., Zhou, S. C., Wu, S. Z. & Wang, H. Inflammasomes and Fibrosis. *Front Immunol* **12**, (2021).

162. Liu, G. *et al.* Therapeutic targets in lung tissue remodelling and fibrosis. *Pharmacol Ther* **225**, (2021).

163. Wilson, M. S. & Wynn, T. A. Pulmonary fibrosis: pathogenesis, etiology and regulation. *Mucosal Immunol* **2**, 103 (2009).

164. Krimmer, D., Ichimaru, Y., Burgess, J., Black, J. & Oliver, B. Exposure to Biomass Smoke Extract Enhances Fibronectin Release from Fibroblasts. *PLoS One* **8**, e83938 (2013).

165. Hu, X., Jiang, C., Hu, N. & Hong, S. ADAMTS1 induces epithelial-mesenchymal transition pathway in non-small cell lung cancer by regulating TGF-β. *Aging* **15**, 2097–2114 (2023).

166. De Arao Tan, I., Ricciardelli, C. & Russell, D. L. The metalloproteinase ADAMTS1: A comprehensive review of its role in tumorigenic and metastatic pathways. *Int J Cancer* **133**, 2263–2276 (2013).

167. Ngassie, M. L. K. *et al.* Age-associated differences in the human lung extracellular matrix. *Am J Physiol Lung Cell Mol Physiol* **324**, L799–L814 (2023).

168. Mejias, N. H., Martinez, C. C., Stephens, M. E., Pablo, J. & Vaccari, D. R. Contribution of the inflammasome to inflammaging. 1–10 (2018).

169. Woldhuis, R. R. *et al.* COPD-derived fibroblasts secrete higher levels of senescence-associated secretory phenotype proteins. doi:10.1136/thoraxjnl-2020-215114.

170. Ahmad, T. *et al.* Impaired mitophagy leads to cigarette smoke stress-induced cellular senescence: Implications for chronic obstructive pulmonary disease. *FASEB Journal* **29**, 2912–2929 (2015).

171. Nyunoya, T. *et al.* Cigarette smoke induces cellular senescence. *Am J Respir Cell Mol Biol* **35**, 681–688 (2006).

172. Kim, S.-Y. *et al.* Mesenchymal stem cell-conditioned media recovers lung fibroblasts from cigarette smoke-induced damage. *Am J Physiol Lung Cell Mol Physiol* **302**, 891–908 (2012).

173. Petrova, N. V., Velichko, A. K., Razin, S. V. & Kantidze, O. L. Small molecule compounds that induce cellular senescence. *Aging Cell* **15**, 999 (2016).

174. Castello, P. R., Drechsel, D. A. & Patel, M. Mitochondria are a major source of paraquat-induced reactive oxygen species production in the brain. *J Biol Chem* **282**, 14186–14193 (2007).

175. Chinta, S. J. *et al.* Cellular Senescence Is Induced by the Environmental Neurotoxin Paraquat and Contributes to Neuropathology Linked to Parkinson's Disease. *Cell Rep* **22**, 930–940 (2018).

176. Woldhuis, R. R. *et al.* COPD-derived fibroblasts secrete higher levels of senescence-associated secretory phenotype proteins. doi:10.1136/thoraxjnl-2020-215114.

177. Traughber, C. A. *et al.* Myeloid-cell-specific role of Gasdermin D in promoting lung cancer progression in mice. *iScience* **26**, (2023).

178. Gao, J. *et al.* Downregulation of GSDMD attenuates tumor proliferation via the intrinsic mitochondrial apoptotic pathway and inhibition of EGFR/Akt signaling and predicts a good prognosis in non-small cell lung cancer. *Oncol Rep* **40**, 1971–1984 (2018).

179. Traughber, C. A. *et al.* Myeloid-cell-specific role of Gasdermin D in promoting lung cancer progression in mice. *bioRxiv* 2022.08.22.504854 (2022) doi:10.1101/2022.08.22.504854.

180. Gene Expression - CZ CELLxGENE Discover. https://cellxgene.cziscience.com/gene-expression.

181. Wu, T. *et al.* Gasdermin-E Mediated Pyroptosis—A Novel Mechanism Regulating Migration, Invasion and Release of Inflammatory Cytokines in Rheumatoid Arthritis Fibroblast-like Synoviocytes. *Front Cell Dev Biol* **9**, (2022).

182. Zhang, Z. *et al.* Caspase-3-mediated GSDME induced Pyroptosis in breast cancer cells through the ROS/JNK signalling pathway. *J Cell Mol Med* **25**, 8159–8168 (2021).

183. Wei, Y. *et al.* GSDME-mediated pyroptosis promotes the progression and associated inflammation of atherosclerosis. *Nature Communications 2023 14:1* **14**, 1–17 (2023).

184. Kawaguchi, M. *et al.* Inflammasome activation of cardiac fibroblasts is essential for myocardial ischemia/reperfusion injury. *Circulation* **123**, 594–604 (2011).

185. Teitz, T. *et al.* Th-MYCN Mice with Caspase-8 Deficiency Develop Advanced Neuroblastoma with Bone Marrow Metastasis. *Cancer Res* **73**, 4086 (2013).

186. Jiang, Z. L., Fletcher, N. M., Diamond, M. P., Abu-Soud, H. M. & Saed, G. M. S-nitrosylation of caspase-3 is the mechanism by which adhesion fibroblasts manifest lower apoptosis. *Wound Repair Regen* **17**, 224 (2009).

187. Peng, X. *et al.* Local apoptosis promotes collagen production by monocyte-derived cells in transforming growth factor β1-induced lung fibrosis. *Fibrogenesis Tissue Repair* **4**, (2011).

188. Martinez, F. J. *et al.* Idiopathic pulmonary fibrosis. *Nature Reviews Disease Primers 2017 3:1* **3**, 1–19 (2017).

189. Badaro-Garcia, S., Hohmann, M. S., Coelho, A. L., Verri, W. A. & Hogaboam, C. M. Standard of care drugs do not modulate activity of senescent primary human lung fibroblasts. *Scientific Reports 2023 13:1* **13**, 1–12 (2023).

190. Dooley, A. *et al.* Modulation of collagen type I, fibronectin and dermal fibroblast function and activity, in systemic sclerosis by the antioxidant epigallocatechin-3-gallate. *Rheumatology* **49**, 2024–2036 (2010).

191. Yang, B. *et al.* Effects of caspase inhibition on the progression of experimental glomerulonephritis. *Kidney Int* **63**, 2050–2064 (2003).

192. Figeac, F. *et al.* Lung Fibroblasts Share Mesenchymal Stem Cell Features Which Are Altered in Chronic Obstructive Pulmonary Disease via the Overactivation of the Hedgehog Signaling Pathway. *PLoS One* **10**, (2015).

193. Togo, S. *et al.* Lung Fibroblast Repair Functions in Patients with Chronic Obstructive Pulmonary Disease Are Altered by Multiple Mechanisms. *Am J Respir Crit Care Med* **178**, 248 (2008).

194. Clifford, R. L. *et al.* Altered DNA methylation is associated with aberrant gene expression in parenchymal but not airway fibroblasts isolated from individuals with COPD. *Clin Epigenetics* **10**, 1–14 (2018).

195. Wan, N. *et al.* Gasdermin D: A Potential New Auxiliary Pan-Biomarker for the Detection and Diagnosis of Diseases. *Biomolecules* **13**, (2023).